

## ***Interactive comment on “Determining the Plio-Quaternary uplift of the southern French massif-Central; a new insights for intraplate orogen dynamics” by Oswald Malcles et al.***

**Oswald Malcles et al.**

oswald.malcles@umontpellier.fr

Received and published: 27 September 2019

Modified manuscript is provided in supplement

Reviewer 1

This article from Malcles et al., presents a nice example of how cosmogenic dating of burial sediments can be used for landscape reconstruction. The multi-methodological approach is particularly interesting, coupling cosmogenic and magnetostratigraphic data with geomorphological analysis and numerical model of lithospheric scale uplift. The article is globally well written and consistently illustrated, even if as I point

Printer-friendly version

Discussion paper



out below, some of the figures can be improved to provide a better understanding of the different datasets. The paper is reasonably organized; the data are produced and interpreted state-of-the-art and the line of arguments is generally consistent and convincing, and supports discussion and conclusions. However, some improvement is required with respect to a couple of problems, such as the erosion trend used as input data in the numerical model. The paper of Malcles et al. contributes substantially to reconstruct the landscape evolution and uplift history of the French Massif Central. The paper fits excellently in the profile of Solid Earth, and I would suggest publication after moderate modifications. Some general suggestions are listed below, and are complemented by specific comments in the attached pdf text file.

Q1: My main remark is related in the interpretation of the onset of the regional uplift. I find that the data well constrain the Plio-Quaternary incision rates but the onset of the uplift is not well demonstrated.

A1: Although we agree with the reviewer #1, the time period covered by our samples is unfortunately following the onset of the uplift and any conclusion on the onset of the uplift would be nothing more than an hypothesis loosely supported by the data. For instance, the area is part of the lithospheric-scale structure which is the Massif Central and it makes sense that the local evolution is linked to the regional evolution. We agree that this question is important to address for a better understanding of the regional dynamic, and hence, for stable continental area deformation driving processes, but it is out of the scope of the paper. We made it clearer in the paper. Line 59-60: adding "Further studies should aim to address the problem of uplift onset, giving more clues concerning the stable continental area but owing the data we presently have, discussing such onset is out of the scope of the paper."

Q2: Introduction The introduction does not follow a classical organization, and introduction is merged with the tectonic setting and with the list of hypothesis to prove. I do not dislike it, but I suggest to separate in a sub paragraph the discussion of the hypothesis that the authors want to test.

A2: In order to make it clear, we split the Introduction in two parts: 1.1 Introduction (line 36) and 1.2: Working hypothesis (line 95)

Q3: About the three scenarios proposed I would like address your attention on the case of old uplift. The uplift could have started early and you could record only the last <5 Ma history of incision, a probably increase in the incision rates. The attached sketch explain the two alternative scenario and a possible relationship with the flat surface.

A3: First, we agree that the incision-rate is probably not linear if looking at higher frequencies, and could have started earlier. For example, such incision-rate variations have been proposed for the Alps (See Saillard et al., 2014; Rolland et al., 2017; Line 386). There is not any possibility to test, based on our data, if there was an increase in the last 5 Myrs, but we can not rule out a marginal increase over the last 5Myrs. Concerning the flat surfaces, we understand this comment as rising the question of possible apparent dip due to diffusion processes and not due to differential uplift. First, we point out that surfaces present southward dipping on both river-sides (if the dipping is due to diffusion processes, we expect dipping toward the river). Second, diffusion processes will mark the surfaces edges first, creating convex topography. This convex shape (and probable increasing dip) would be discarded either by automatic recognition or by manual control of the surface robustness. To take into account this remark we added for clarity: “ Diffusion processes could create apparent tilt of remnant horizontal surfaces. However, we avoid that problem by completing the automatic selection and correction with a final check to make sure that the residuals are randomly distributed over the surface (see below).” (Lines 283-285).

Q4: The age and the geological meaning of the flat upper surface is relevant to reconstruct the onset of uplift.

A4: Agree, but because of the strong uncertainties concerning the ages of the upper surface (e.g. possible important time-lag between the surface formation and the uplift onset), we chose not to discuss it in the paper that deals mainly with the Plio-

[Printer-friendly version](#)[Discussion paper](#)

Quaternary dynamic.

Q5: Moreover, the relationship of the cave galleries with the upper flat surface and with the geomorphological markers should be better described. Karst model One of the main point in using the cave galleries as ancient base level is to show that cave passages were really connected to the base level and that they are not only a perched level of preferable karst dissolution. For this reason I would like to see the profiles of the cave systems and its relationship with the river and eventually some photos testifying the phreatic style of the passages.

A5: We agree with possible alteration-driven karstification but, we do not propose to discuss the cave formation. Indeed, to our knowledge, there is no way to date the void created by karst galleries, therefore we use them only as empty pockets trapping sediments without any doubt, and now located on canyon wall as already done by Granger et al., (1997, 2001). This is the case at least for the Rieutord caves and the Garrel, for the Leicasse cave we refer the reader to Camus (2003) where the link to fluvial transport has been shown. Therefore, we think that adding more pictures of the caves and figures would not bring a significant gain in clarity. We refer the reader to publication where these relations are discussed e.g. Audra et al., (2001) or Moccochain (2007) and the link to fluvial transport has been shown (Camus, 2003). To allow the reader to have a look at the geometry of the caves we added a link to a university hosted database with a doi where the caves are available in 3D. Line 1548-154: Karst3D (2019). Karst3D data base. <https://doi.org/10.15148/940c2882-49f1-49db-a97e-12303cace752>

Q6: Why haven't you dated samples from the Leicasse cave, that is placed at high elevation? Higher levels exist (between 600 and 700 m) in the same region suggesting an old history of the uplift and incision.

A6: Dating of other samples is in progress and should be subject to publication when obtained. Furthermore, we point out that to our knowledge quartz bearing infilling are

Printer-friendly version

Discussion paper



not present at 600-700m a.s.l. In the explored caves. Highest known quartz cobbles in the Leicasse cave are located c.a. 450 a.s.l.

Q7: To show the sampling sites within the caves and the location of the caves on the topographic maps could help the reader.

A7: See above for topographic survey database. (Sampling site will be added).

Q8: Geomorphological analysis I found this part interesting and useful to put quantitative data in a regional scenario. I have some doubts about the paragraph organization: the three working hypothesis shown at the beginning seem a bit extraneous in a paragraph where the authors should explain how to extract the data and show the results. I suggest to rethink this organization.

A8: The paragraph structure has been rewritten in order to make it clear with in order: methods, expectations and results. Line 257 to 267 have been moved to Line308-320.

Q9: Also the title of the paragraph seems a bit out of context, better “analysis” instead of “evidences”, for example.

A9: Changed to “Geomorphometrical approach” Line 276.

Q10: I wonder to see some pictures of the analyzed and discussed markers.

A10: We added as supplementary some pictures of the discussed flat surfaces.

Q11: The limit of 2° of slope is questionable. For me the problem is the topographic gradient of the entire margin. Along a NNW-SSE directed profile from Aigoual summit to the Cevennes fault the mean gradient is about 2°, with important local variations that show topographic gradient up to 4° (few kilometers SE to the summit of the Mt Aigoual for example). I would like to see if tilted plans between 2° and 4° exist. The limit of 2° is reasonable for Plio-Quaternary marker, but it is possible that older geomorphological marker could be more tilted.

A11: We agree that using 2° as slope cut-off will limit the detection of some surfaces

[Printer-friendly version](#)[Discussion paper](#)

and lead to miss some markers. But we focus on the Plio-Quaternary evolution, therefore the 2° cut-off could even be seen as a proxy for older (and polyphased) surface filter. For instance, old surface in the Larzac plateau have been proposed by Bruxelles (2001) but we didn't include them in our analysis because of their expected old ages and so forth, possible strong alterations, plural-deformation registration, etc.

Q12: How the slope of each marker have been calculated?

A12: As explained in lines 280-302 we use automatic and manual delimitation of surface, iterative plan fitting using extracted DEM points and statistical outliers suppression, and robustness criterions filter. We have modified these lines to make it clearer.

Q13: Numerical modeling The approach is interesting and perfectly reasonable even if I am not the right person to evaluate the details. However, I have some remarks on the input data for the modeling. The authors used a regional distribution of erosion that do not correspond exactly to the published data. In figure 11 the maximum of erosion is placed at the top the Mt Aigoual, with value of 0.08 mm/yr (or 80 m/Myr) (please, change the dimension to homogenize text and figure). But, the values on top reach the minimum values testified also by the oldest thermochronological ages (long-term erosion) of Barbarand et al., 2001 and Gautheron et al., 2009. Also the cosmogenic denudation rates of Olivetti et al. 2016 suggest that the erosion on the top of the massif close to the margin is very limited (values of about 0.04 mm/yr). The values increase along the flank, toward the lower elevation samples, confirmed by your new data set of incision rates.

A13: Dimensions in figure have been changed for consistency. We extended the explanations in the text to explain the erosion-profile setting (lines 352-360): "This profile is a simplification of the one that can be expected from Olivetti et al. (2016) and do not aim at matching precisely the published data because of, first, the explored time-span (~ 1 Myrs) is not covered by thermochronological data (> 10Myrs) or cosmogenic denudation rate (10s-100s kyrs). Second, we assume that erosion rates are correlated to

Printer-friendly version

Discussion paper



the first order to the local (10s km<sup>2</sup>) slopes, that are higher near the drainage divide. This allows to include any kind of erosion processes (e.g. landslides). Third, the model supposes a cylindrical structure perpendicular to the cross section, this implies to average the high-frequency lateral variations of slope, elevation, etc. to derive the actual denudation rate based on these proxies. Concerning this erosion profile, a parametric study with highest erosion rate ranging from 1 to 1000 m.Myrs<sup>-1</sup> led to the same first order interpretations..”

Q14: Therefore, the input data of the erosion distribution that the authors used for the modeling is a bit different from the measured data. I think that an erosion trend resulting bigger at lower elevation and minor at high elevation is not consistent with a process of isostatic uplift induced by erosion, supporting event more clearly the authors conclusions.

A14: Using numerous erosion profiles, but with always a pattern of erosion on the relief and deposit off-shore won't change the first order results since they are mainly controlled by the Elastic parameters. We extended description of the choice of the erosion profile to make it clear (lines 352-360. (See A13 above).

Q15: I suggest to be more rigorous in the description of the geodynamic model: for instance the flexural response to the gulf of Lion extension is complicated to invoke, for the distance between the high topography and basin. The role of the mantle upwelling has been proposed by many authors (that have to be cited) that worth to be discussed a bit more in detail (dynamic or isostatically supported, the Massif Central thin lithosphere suggests, in my opinion, a clear contribution of the mantle in the present topography).

A15: We agree that mantle or deep processes are involved in the uplift onset. However, we developed a conceptual to test the role of the erosion-induced isostatic adjustment and not to elaborate more complicated models with too many parameters compared to the constraints that we have. For instance, we cannot decipher if the thin and slightly hot lithosphere is related to dynamic topography with ongoing mantle upwelling or if it

[Printer-friendly version](#)[Discussion paper](#)

is supported by thermal isostasy being a remnant of past processes like the opening of the Gulf of Lion.

Discussion Q16: Lines: 376 is not clear for me.

A16: “Hence, the incision rate has to be balanced to the first order by the uplift rate”. Explanation has been added for better clarity Lines 420 – 424: “Hence, back to the three conceptual models presented in part 1 (Fig.2), we can discard, at first order, the models A (Old uplift-recent incision) and B (Old uplift-old incision) because the obtained incision rate shows recent incision and surface tilting tend to prove a current uplift. Therefore, the incision rate has to be balanced to the first order by the uplift rate. Eustatic variations magnitudes are of too low (100-120 m) to explain the total incision (up to 400m). “

Q17: The only way that I know to re-equilibrate a river profile is a regressive erosion that move from the base level upstream. If the river is full equilibrated means that regressive erosion reached the uppermost part of the profile. Moreover the lack of knickpoint does not prove that incision rate and uplift are in equilibrium, if the landscape undergoes a long topographic degradation.

A17: We agree that the lack of knickpoints do not prove an equilibrium state (and that in general the term “equilibrium” is subject to debate) but it allows to dismiss a strong impact of regressive erosion due to recent sea-level variations or tectonic. To address the concern of long topographic degradation (assuming no uplift?), we point out that such degradation will lead to mass export, then lithospheric unloading and then isostatic-adjustment uplift, which is why we developed our conceptual model to test if this process could be responsible for our observations.

Q18: It could be interesting to know why the rivers profiles from northeastern margin of the Massif (Olivetti et al.) and from Ardeche (personal data) show knickpoints and Cevennes rivers not. If the authors want to discuss about the river profiles it could be interesting to show some data.

[Interactive comment](#)

[Printer-friendly version](#)

[Discussion paper](#)



A18: This subject looks important and further study should be addressed in this sense. But discussion about the river profiles are beyond the scope of this paper and seems to us unnecessary, especially in a manuscript that is already long and complex. Indeed, for drawing robust conclusions, we should, as suggested by Reviewer #1 enlarge the study to other rivers surrounding the Massif Central and not only the ones in our study. As Reviewer #1 we noticed the difference in knickpoints between the southern and eastern margin of the Massif-Central and we think that it deserves a more complete study, notably to discuss a possible role of karstic dynamic given the major lithological difference between these two regions.

Q19: Onset of volcanism is placed about 13 Ma and even earlier if we consider the synrift volcanism (Michon and Merle 2001).

A19: We agree, according to Nehlig et al., the volcanism started 65 Ma ago in some places. One of the many issues they highlighted was the diachronism of the volcanic activity throughout the Massif-Central. For example, they show an activity spanning from 13 to 2 Ma with a paroxysm at 8.5 Ma for the Cantal stratovolcano. Dautria et al. (2010) proposed younger ages of volcanic structures southward, etc. We chose 5 Ma as an average of increased activity throughout the area but not as the onset of the volcanisms which is on the other hand of major importance in the discussion of the uplift onset, as previously discussed.

Q20: Figures: In general the figures are good, but sometimes they lack of useful information such as topographic names (summits, cities, etc). I would appreciate to see the location of the analyzed caves in a map (in the figure 9 for example) and also the profile in a vertical view of the caves to have a look of the general topographic trend, its relationship with the incised river, and to show the sampling sites.

A20: Changed accordingly with some geographical information, trying not to overload the figures. See modified figure.

Q21: Coordinates are lacking.

[Printer-friendly version](#)[Discussion paper](#)

A21: Lacking coordinates are now provided in the figure 1 caption.

Figure 3 and 4 could be merged. Please also note the supplement to this comment: <https://www.solid-earth-discuss.net/se-2019-99/se-2019-99-RC1-supplement.pdf> Modifications included, and answer in the section below.

Supplementary review 1:

SQ1: Line 43: I agree with the recent uplift, but it is still under debate. The topography could be also interpreted as a longlasting degradation of an ancient topography.

SA1: We agree. This hypothesis is presented latter in this section. We changed the sentence in order to present it as our chosen hypothesis but not the unique one possible.

SQ2: Line 58: 9 kms seem a bit too much, anyway big thickness is found in the de-pocenter basin, such as the center of Ales Basin, while along the Cevennes margin the thickness progressively decrease toward the NW. It is not proven that the entire Cevennes region was covered by Mesozoic sediments.

SA2: Noted and slight changes in the sentence (“reach several kilometers” instead of “be more than 9km”. The 9 kms are for the overall SE basins (southward of Ales Basin). Anyway, exact spatial coverage or thickness will not change our point given that the first order is sufficient to our study.

SQ3: Line 60: The uplift event is called Durancian uplift event while the Isthmus is the topographic high formed as a consequence, I think.

SA3: Noted and changed accordingly.

SQ4: Line 69: do you refer to Sanchis and Seranne?

SA4: Indeed, as an example of evolution induced by the extensional period, not as direct study of the watershed evolution.

Printer-friendly version

Discussion paper



SQ5: Line 70: To be meticulous, the events are three: the Mid-cretaceous uplift, the Pyrenean compression and the Oligocene extension.

SA5: We agree. The Durancian event (Mid-Cretaceous uplift) is presented before in the section but should be mentioned here. Changed accordingly.

SQ6: Line 93:

SA6: Tilt → Tilting

SQ7: line 55-56: I suggest to use Ma instead of Myrs ago

SA7: Changed accordingly.

SQ8: Line 132: It could be useful for the readers a briefly description of the morphological setting of the area, with the plateau, canyons ect.

SA8: Short descriptions are provided Line 54 to 59. We added call to figure 1 (for the provided topographic map) for visual insights into first order morphology.

SQ9: Line 136: sequence

SA9: Changed accordingly

SQ10: Line 140:

SA10: References writing changed

SQ11: Line 154:

SA11: Some precisions concerning the sediments protolith area are now provided.

SQ12: Line 594: fig. 9.

SA12: Changed accordingly

SQ13: Figure 1: It is not very clear the location of the Massif Central. It could be interesting to see the sampling location divided for methods, where you performed

[Printer-friendly version](#)[Discussion paper](#)

cosmogenic analysis and where paleomagnetism.

SA13: Context map was changed with zoom over western Europe. More information added into the figure caption. See revised figure.

SQ14: Figure 11: change mm.yr-1 in m.Myr-1 "the studied area that include the studies zones" sounds a bit as tautology. It could be better to clarify. the simbol v is gone

SA14: Dimensions changed for consistency to m.Ma-1. Unclear sentence was removed. Symbol v has been added.

Please also note the supplement to this comment:

<https://www.solid-earth-discuss.net/se-2019-99/se-2019-99-AC1-supplement.pdf>

---

Interactive comment on Solid Earth Discuss., <https://doi.org/10.5194/se-2019-99>, 2019.

Printer-friendly version

Discussion paper



# ***Interactive comment on “Determining the Plio-Quaternary uplift of the southern French massif-Central; a new insights for intraplate orogen dynamics” by Oswald Malcles et al.***

**Oswald Malcles et al.**

oswald.malcles@umontpellier.fr

Received and published: 27 September 2019

Modified manuscript is provided in supplement.

Q1: This paper presents original data on an interesting geomorphological subject where quantification is difficult and rare. The overall conclusion that South Massif Central has seen an incision and related uplift of about 80 m/Myr in the last 4 Ma, associated with a tilt toward the south is sound and deserves publication. However, the way the data is presented is far from satisfactory (missing information, hard to understand figures, neglected data without justification, etc., see details below) and thus I suggest important revisions to be performed before acceptance. English needs also

Printer-friendly version

Discussion paper



significant improvement. I point a few points below.

A1: We took into consideration your comments and suggestions. We hope that our revisions and our answers below will clarify our work. The English has been reviewed. We would like to emphasize that one of the authors is a native English speaker (Australia).

Q2: details “ $83.4+17.3/-5.4$ ” is too precise!  $83+17-5$  is enough. . .

A2: Agree, and change accordingly.

Q3: Burial dating using Terrestrial cosmogenic nuclides (TCN) are nowadays: change are to is. Line 38 (and elsewhere): “can’t” cannot is more advisable.

A3: Corrected

Q4: Fig.1 lacks latitude longitude and some landmarks (even myself who works in the area was not sure to locate the main structures) like main rivers, cities, . . .

A4: Additional information has been added to the map, trying to find a balance between information and clarity. See revised figure.

Q5: A geological map could be useful.

A5: At the scale of the study region and given the topic of the manuscript, we think that a topographic map is much more useful than a geological map to observe the overall morphology (besides, we mentioned clearly in the introduction and the tectonic setting that the geology of the studied area corresponds mainly to Mesozoic to lower Cenozoic limestones plateaus).

Q6: Also the localization of studied sites is poorly precised in this figure.

A6: Given the scale of Figure 1, it is not possible to locate precisely the studied points. We gave their precise geographical coordinates in the figure captions.

Q7: Could they be also indicated in e.g. fig.9?

A7: Yes, we added them.

Q8: Line 123-124: sentence needs a verb!

A8: “Creating” changed to “creates”.

Q9: Line 166-169 : strange practice to give results in the methods section (2.1) Please move them to section 2.2!

A9: We did it (see revised manuscript lines 211-214)

Q10: Line 216:  $83 \pm 35$  is enough precise. A table of paleomagnetic results with statistical parameters is mandatory. A10: We added the table in the supplementary material.

Q11: Fig.6 is hard to understand (especially not knowing how much paleomagnetic sites are available). I figure that on paleomag polarity is represented arbitrarily by a set of points fitted with chosen incision rate, allowing to see if the polarity is consistent with the scale, indicated as vertical grey strips. This is very badly explained !

A11: Almost all the part 2.2.2, the figure and the captions have been reworked for better clarity.

Q12: Line 219 “First, we note a good agreement between samples located at the same elevation,” I really don’t get how you derive such assertion!

A12: We added explanation Line 2541-242: “samples located at the same elevation and being part of the same stratigraphic layer (Camus, 2003). This syngenetic deposition allow, as best explanation to prevent from a possible partial endokarstic reworking”. Indeed, Some sampling sites are located at slightly different elevation but inside the same gallery and, as part of the same sedimentary layer they have to display the same polarity, that is the case. This consistency is not on its own a proof that the clay didn’t sediment in different period (with same polarity) but it is by far the most reasonable explanation. See supplementary material with analysis details.

Q13: Line 223-225: about this reverse-normal sequence, there is no way to see it on Fig.6! Again the table is mandatory! You have to comment on the reverse polarity at

[Printer-friendly version](#)[Discussion paper](#)

≈40 m that you assign to Brunhes period. Why not putting Matuyama there?

A13: Given the poor quality of the data, we skipped it from the interpretation. See supplementary material.

Q14: Line 243: “Using a similar approach for the Rieutord crystalline samples,” I don’t get what you mean!

A14: We added simple explanations in the paragraph: “Using a similar approach for the Rieutord crystalline samples where we minimize the residual between the observed and the modeled ages based on the same incision-rate range than for the paleomagnetic samples”.

Q15: How do you compute average dip and azimuth of your geomorphological surfaces? If it’s arithmetic mean, that not acceptable. You have to make it using directional statistics (and show us a stereogram of dip lines)

A15: Given values are indeed not arithmetic mean. We checked again the computation and minor errors have been fixed (Average dip changed from  $0.61 \pm 0.41^\circ$  with an azimuth of  $N150 \pm 40^\circ E$  tot  $0.60 \pm 0.40^\circ$  with an azimuth of  $N128 \pm 36^\circ E$ ). It does not change the interpretation. Errors was due to mistake in downward sign for 2 surfaces. Because of very low dip angle of the plane, the conventional representation through stereogram is useless and won’t provide the information brought by the histograms.

Q16: Is Fig.9 all markers or only the robust ones? The second option (38 data; but I count 45 on fig.9!) seems right. But then the azimuths exhibit in fig.9 does not fit Fig.10. There are northward dips!

A16: Fig. 9 doesn’t display only the robust values. We added different color in order to decipher in between the two sets. Note that some surfaces cannot be shown on the map because of their small size and their closeness. See revised figure 9.

Fig.10 scale “surface density” is a number of surfaces? Please make this clear.

[Printer-friendly version](#)[Discussion paper](#)

A10: Yes. Modified accordingly.

Please also note the supplement to this comment:

<https://www.solid-earth-discuss.net/se-2019-99/se-2019-99-AC2-supplement.pdf>

Interactive comment on Solid Earth Discuss., <https://doi.org/10.5194/se-2019-99>, 2019.

SED

Interactive  
comment

Printer-friendly version

Discussion paper



1 Determining the Plio-Quaternary uplift of the southern French massif-Central; a new insights for in-  
2 traplate orogen dynamics.

3 Oswald Malcles<sup>1</sup>, Philippe Vernant<sup>1</sup>, Jean Chéry<sup>1</sup>, Pierre Camps<sup>1</sup>, Gaël Cazes<sup>2,3</sup>, Jean-  
4 François Ritz<sup>1</sup>, David Fink<sup>3</sup>.

5 <sup>1</sup>Geosciences Montpellier, CNRS-University of Montpellier, Montpellier, France

6 <sup>2</sup>SEES, University of Wollongong, Wollongong, Australia

7 <sup>3</sup>Australian Nuclear Science and Technology Organisation, Lucas Heights, Australia

8 *Correspondence to:* Oswald Malcles (oswald.malcles@umontpellier.fr)

## 9 **Abstract.**

10 The evolution of intra-plate orogens is still poorly understood. Yet, this is of major importance for understand-  
11 ing the Earth and plate dynamic, as well as the link between surface and deep geodynamic processes. The  
12 French Massif Central is an intraplate orogen with a mean elevation of 1000m, with the highest peak elevations  
13 ranging from 1500m to 1885m. However, active deformation of the region is still debated due to scarce evi-  
14 dence either from geomorphological or geophysical (i.e. geodesy and seismology) data. Because the Cévennes  
15 margin allows the use of karst sediments geochronology and morphometrical analysis, we study the vertical dis-  
16 placements of that region: the southern part of the French Massif-Central. Geochronology and morphometrical  
17 results, helped with lithospheric-scale numerical modelling, allow, then, a better understanding of this intraplate-  
18 orogen evolution and dynamic.

19 Using the ability of the karst to durably record morphological evolution, we first quantify the incision  
20 rates. We then investigate tilting of geomorphological benchmarks by means of a high-resolution DEM. We fi-  
21 nally use the newly quantified incision rates to constrain numerical models and compare the results with the ge-  
22 omorphometric study.

23 We show that absolute burial age (<sup>10</sup>Be/<sup>26</sup>Al on quartz cobbles) and the paleomagnetic analysis of karstic clay  
24 deposits for multiple cave system over a large elevation range correlate consistently. This correlation indicates a  
25 regional incision rate of  $83.4^{+17.3}_{-5.4}$  m.Ma<sup>-1</sup> during the last ca 4 Myrs (Plio-Quaternary). Moreover, we point out  
26 through the analysis of 55 morphological benchmarks that the studied region has undergone a regional south-  
27 ward tilting. This tilting is expected as being due to a differential vertical motion between the north and southern  
28 part of the studied area.

29 Numerical models show that erosion-induced isostatic rebound can explain up to two-thirds of the regional up-  
30 lift deduced from dating technics and are consistent with the southward tilting obtain from morphological analy-  
31 sis. We presume that the remaining part is related to dynamic topography or thermal isostasy due to the Massif  
32 Central plio-quaternary magmatism.

## 33 **1 Introduction and Tectonic Setting**

### 34 1.1 Introduction

35 Since the past few decades, plate-boundary dynamics is to a first order, well understood. Such is not the case for  
36 intraplate regions, where short-term (10<sup>3</sup>-10<sup>5</sup> yrs.) strain rates are low and the underlying dynamical processes

37 are still in debate (e.g. Calais et al., 2010; Vernant et al., 2013; Calais et al., 2016; Tarayoun et al., 2017). On ge-  
38 ological time-scales, transient phenomenon that are classically used to explain intraplate deformations (as seen  
39 through the seismic activity) can<sup>2</sup> ~~not~~ be a satisfactory explanation though, this then raises the question of the  
40 origin of the high finite deformations observed in many parts of the world as for instance the Ural mountains in  
41 Russia, the Blue Mountains in Australia or the French Massif Central.

42 In this study we focus on the Cevennes Mountains and the Grands Causses regions that form the southern part  
43 of the French Massif Central, located in the southwestern Eurasian plate (fig.1). The region is characterized by a  
44 mean elevation of 1000 m with summits higher than 1500 m. Such topography is likely to be the result of recent,  
45 active uplift and as the Cevennes mountains experiences an exceptionally high mean annual rainfall (the highest  
46 peak, Mount Aigoual, records the highest mean annual rainfall in France of 4015 mm) it raises the question of a  
47 possible link between erosion and uplift as previously proposed for the Alps (Champagnac et al., 2007; Vernant  
48 et al., 2013; Nocquet et al., 2016). This region currently undergoes a small but discernible deformation, but no  
49 significant quantification can be deduced due to the scarcity in seismicity (Manchuel et al., 2018). In addition,  
50 GPS velocities are below the uncertainty threshold of GPS analyses (Nocquet et Calais, 2003; Nguyen et al.,  
51 2016).

52 South and West of the crystalline Cevennes mountains, prominent limestone plateaus, named Grands Causses,  
53 rise to 1000m and are dissected by ~~fewseveral~~ canyons that are several hundreds of meter deep (Topographic  
54 font in figure 1 show first order topography and morphology). The initiation of incision, its duration and the ge-  
55 omorphic processes leading to the present-day landscape remain poorly constrained. A better understanding of  
56 the processes responsible for this singular landscape would bring valuable information on intraplate dynamics,  
57 especially where large relief exists.

58 The oldest formations in the area were formed during the Variscan orogeny (late Palaeozoic, ~300 M~~yr~~s-~~ago~~a; ~~ago~~a;  
59 Brichau et al., 2007) and constitute the crystalline basement of the Cevennes. Between 200 and 40 M~~yr~~s-~~ago~~a  
60 (Mesozoic and lower Cenozoic), the region was mainly covered by the sea ensuring the development of an im-  
61 portant detrital and carbonate sedimentary cover, which can ~~reach several~~be more than 9 km thick in some loca-  
62 tions (Sanchis and Séranne, 2000; Barbarand et al., 2001). During the Mesozoic era, an episode of regional up-  
63 lift and subsequent erosion and alteration (called the Durancian ~~isthmusevent~~) is proposed as being at the origin  
64 of the flat, highly elevated surface that persists today across the landscape (Bruxelles, 2001; Husson, 2014).

65 The area is also affected by the major NE-SW trending Cevennes fault system. During the Pyrenean orogeny, 85  
66 to 25 Ma (Tricart, 1984; Sibuet et al., 2004), several faults and folds affected the geological formations south of  
67 the Cevennes fault, while very few deformations occurred further north within the Cévennes and Grand Causses  
68 areas (Arthaud and Laurent, 1995). Eventually, the Oligocene extension (~30 M~~yr~~s-~~ago~~a) led to the counter-  
69 clockwise rotation of the Corso-Sardinian block and the opening of the Gulf of Lion, re-activating some of the  
70 older compressive structures as normal faults. The main drainage divide between the Atlantic Ocean and the  
71 Mediterranean Sea is located in our study area and is inherited from this extensional episode (Séranne et al.,  
72 1995; Sanchis et al., 2000).

73 Superimposed at the inheritance from Durancian event, the last ~~These~~ two major tectonic episodes which are the  
74 (Pyrenean compression and the Oligocene extension ~~are the main geodynamic processes that~~) shaped the large-  
75 scale structural morphology of the region. Afterwards during the Plio-Quaternary period, only intense volcanic  
76 activity has affected the region, from the Massif Central to the Mediterranean shoreline. This activity is charac-

77 terised by several volcanic events that are well constrained in age (Dautria et al., 2010). The last eruption oc-  
78 curred in the Chaîne des Puys during the Holocene (i.e. the past 10 kyrs (Nehlig et al., 2003; Miallier et al.,  
79 2004). Some authors proposed that this activity is related to a hotspot underneath the Massif Central (Granet et  
80 al., 1995; Baruol and Granet, 2002) leading to an observed positive heat-flow anomaly and a possible regional  
81 plio-Quaternary uplift.

82 Despite this well described overall geological evolution the onset of active incision that has shaped the  
83 deep valleys and canyons (e. g. Tarn or Vis river, Fig 1) across the plateaus, and the mechanisms that controlled  
84 this incision are still in debate. One hypothesis proposes that canyon formation was driven by the Messinian  
85 salinity crisis with a drop of more than 1000m in Mediterranean Sea level. This, however, would then not ex-  
86 plain the fact that the Atlantic watersheds show similar incision. Other studies suggested that the incision is con-  
87 trolled by the collapse of cave galleries that lead to fast canyon formation mostly during the late Quaternary,  
88 thus placing the onset of canyon formation only a few hundreds of thousands of years ago (Corbel, 1954). In  
89 contrast, it has also been proposed more recently (based on relative dating techniques and sedimentary evidence)  
90 that incision during the Quaternary was negligible (i.e. less than a few tens of meters), and that the regional mor-  
91 phological structures seen today occurred around 10 Myrs-agoa (Séranne et al., 2002; Camus, 2003).

## 92 1.2 Working hypothesis

93 In this paper, we provide new quantitative constraints on both the timing of incision and the rate of riv-  
94 er down-cutting in the central part of the Cévennes and of the Grands Causses that has resulted in the large relief  
95 between plateau and channel bed. We employ two methods, cosmogenic  $^{10}\text{Be}/^{26}\text{Al}$  burial dating quartz cobbles  
96 that have been transported by rivers and paleomagnetic analyses along vertical profiles of endokarstic clay both  
97 of which have been deposited in multiple cave systems at the time cave entry was at river channel elevation. In  
98 parallel, by analysing a high-resolution DEM (5m), we show that the region is affected by a regional tilt [ing](#). Our  
99 results allow to quantify the role of the Plio-Quaternary incision on the Cévennes landscape evolution and to  
100 constrain numerical modelling from which we derive the regional uplift rates and a tilt of geomorphological  
101 markers.

102 One important point of this study is the integration of multi-disciplinary approaches in order to con-  
103 strain intraplate deformation. Such an approach is necessary to bring new insights into the lithosphere behaviour  
104 of slow dynamic regions. If the uplift is easily recognisable in the landscape (1000 m high plateaus), quantifying  
105 its timing and evolution rates is harder and can't be performed by classical technics (e.g. GPS). This is why we  
106 aim to quantify the incision rate over the longest possible period thanks to the karstic immunity. Dealing with  
107 long-term incision rates (up to 5 Myrs) should permit to smooth possible climatic-driven incision rate variations  
108 (with time-span of several kyrs)..

109 If incision is initiated by uplift centred on the North of the area where elevations are maximum, it will lead to  
110 tilting of fossilised topographic markers as strath terraces. Our method of analyses provides an opportunity to  
111 select between three possible explanations for the current terrain morphology. The first is based on old uplift  
112 and old incision (Fig. 2.A). In this case, apparent incision rates would be very low. For instance, if incision com-  
113 menced 10 Myrs-agoa (Serrane et al., 2002), we would find surface tilting but cosmogenic burial dating with  
114  $^{10}\text{Be}/^{26}\text{Al}$  which cannot discern ages older than  $\sim 5\text{Ma}$  due to excessive decay of  $^{26}\text{Al}$ , would not be possible.  
115 The second possibility (Fig. 2.B) is that the uplift is old, and incision consequently follows but with a time lag.

116 Here the incision rate would be rather fast but no tilting is expected for the river-related markers because no dif-  
117 ferential uplift occurs after their formation. Finally, the third possibility (Fig 2.C) is that uplift and incision are  
118 concurrent and recent (i.e. within the time scale of cosmogenic burial dating) and thus we would expect burial  
119 ages < 5 Myrs relatively high incision rates, and tilting of morphological markers. These different proposals for  
120 the temporal evolution of the region will then be compared using numerical modelling.

## 121 **2. Determining the incision rates in the Cévennes and the Grand Causses Region**

### 122 **2.1. Principles and methods**

#### 123 **2.1.1. Karst model**

124 No evidence of important aggradation events has been reported in the literature for the studied area. Therefore  
125 we base our analysis on a per descensum infill model of the karst networks whereby sediments are transported  
126 and then deposited within cave galleries close to base level. When cave-systems and entry passages are near the  
127 contemporaneous river channel elevation (including higher levels during floods), the deposition into caves of  
128 sediments, from clay to cobbles occurs, especially during flood events. ~~With~~ subsequent river incision into  
129 bedrock creating a relative base level drop (due to uplift or sea-level variations). The galleries associated with  
130 the former base-level are now elevated above the new river course and become disconnected from further depo-  
131 sition. Hence fossilised and trapped sediments throughout the cave network represent the cumulative result of  
132 incision. In this commonly used model (Granger et al., 1997; Audra et al., 2001; Stock et al., 2005; Harmand et  
133 al., 2017), the higher the gallery elevation (relative to the present-day base level) the older the deposits in that  
134 gallery. As a result, the objective here is to quantify a relative lowering of the base level in the karst systems,  
135 with the sediments closest to the base level being the youngest deposits, and note that we do not date the cave  
136 network creation which may very well pre-date river sediment deposition.

137 Within individual canyons, successions of gallery networks across the full elevation range from plateau top to  
138 modern river channel, were not always present and often sampling could not be conducted in a single vertical  
139 transect. Thus we make the assumption of lateral altitudinal continuity i.e. that within a watershed, which may  
140 contain a number of canyons, the sediments found in galleries at the same elevation were deposited at the same  
141 time. Inside one gallery, we use the classical principle of stratigraphy sequence (i.e. the older deposits are below  
142 the younger ones). More informations and detailed relationship concerning the karstic development and geomet-  
143 ric relationship between karstic network and morphological markers could be find in Camus (2003) ~~or #####~~. In  
144 any cases, our aim is not to date the galleries formation, neither to explain the formation processes (e.g. past  
145 preferential alteration layer); but to use the time information brought by the sediment that have been trapped into  
146 the cave system. Therefore, we apply the common used model (example in Harmand et al., 2017) that had been  
147 proved by Granger et al., (1997, 2001 ). For cave topographic survey, we refer the reader to  
148 [https://data.oreme.org/karst3d/karst3d\\_map](https://data.oreme.org/karst3d/karst3d_map) providing 3D survey.

#### 149 **2.1.2. Burial ages**

150 Burial dating using Terrestrial cosmogenic nuclides (TCN) ~~isare~~ nowadays a common tool to quantify incision

151 rates in karstic environment (Granger ~~and~~ Muzikar, 2001; Stock et al., 2005; Moccochain., 2007; Tassy et al.,  
152 2013; Granger et al., 2015; Calvet et al., 2015; Genti, 2015; Olivetti et al., 2016; Harmand et al., 2017; Rovey II  
153 et al., 2017; Rolland et al., 2017; Sartégou, 2017; Sartégou et al., 2018). This method relies on the differential  
154 decay of TCN in detrital rocks that were previously exposed to cosmic radiation before being trapped in the  
155 cave system. With this in mind, the  $^{10}\text{Be}$  and  $^{26}\text{Al}$  nuclide pair is classically used as (i) both nuclides are pro-  
156 duced in the same mineral (i.e. quartz), (ii) their relative production ratio is relatively well constrained (we use  
157 here a standard  $^{26}\text{Al}/^{10}\text{Be}$  pre-burial ratio of 6.75, see Balco et al., 2008) and (iii) their respective half-lives  
158 (about 1.39 Myr and 0.70 Myr for  $^{10}\text{Be}$  and  $^{26}\text{Al}$ , respectively) are well suited to karstic and landscape evolution  
159 study, with a useful time range of  $\sim 100$  ky to  $\sim 5$  Myr.

160 To quantify the incision rate of the limestone plateau of the Cevennes area, we analysed quartz cobbles infilling  
161 from four caves of the Rieutord canyon (Fig. 1), this canyon is well suited for such study because horizontal  
162 cave levels are tiers over 200 m above the current river-level and are directly connected to the canyon, leading  
163 to a straight relationship between river elevation and the four cave infilling that we have sampled (Cuillère cave,  
164 Route cave, Camp-de-Guerre cave and Dugou cave). Furthermore, cobbles source is well known and identified:  
165 the upstream part of the Rieutord river, some tens of kilometres northward, providing a ~~uniform~~unique sediment  
166 origin composed of granite and metamorphic rocks embedding numerous quartz veins. All samples (Example  
167 Fig. 3) were collected far enough away ( $>20\text{m}$ ) from the cave entrance and deep enough below the surface  
168 ( $>30\text{m}$ ) to avoid secondary in-situ cosmogenic production of  $^{10}\text{Be}$  and  $^{26}\text{Al}$  in the buried sediments.

169 The quartz cobbles were first crushed and purified for their quartz fraction by means of sequential acid attack  
170 with Aqua-Regia ( $\text{HNO}_3 + 3\text{HCl}$ ) and diluted Hydrofluoric acid (HF). Samples were then prepared according to  
171 ANSTO's protocol (see Child et al. 2000) and  $\sim 300\mu\text{g}$  of a  $^9\text{Be}$  carrier solution was added to the purified quartz  
172 powder before total dissolution. AMS measurements were performed on the 6MV SIRIUS AMS instrument at  
173 ANSTO and results were normalised to KN-5-2 (for Be, see Nishiizumi et al., 2007) and KN-4-2 (for Al) stan-  
174 dards. Uncertainties for the final  $^{10}\text{Be}$  and  $^{26}\text{Al}$  concentrations include AMS statistics, 2% (Be) and 3% (Al) stan-  
175 dard reproducibility, 1% uncertainty in the Be carrier solution concentration and 4% uncertainty in the natural  
176 Al measurement made by ICP-OES, in quadrature. Sample-specific details and results are found in table 1.

177 ~~and  $0.21 \pm 0.1$  Myrs respectively.  $0.97$ ,  $0.63 \pm 0.37$ ,  $0.95 \pm 0.14$~~ For the four caves, we observed a good relation-  
178 ship between burial ages and incision, except for the Camp-de-Guerre cave (CDG) site, the higher the cave is,  
179 the older the burial ages are. Burial ages for the Cuillère cave, Dugou cave, Camp-de-Guerre cave and Route  
180 eave are  $2.16 \pm 0.15$

### 181 2.1.3. Paleomagnetic analysis

182 In parallel with burial dating, we analyzed the paleomagnetic polarities within endokarstic clay deposits  
183 ~~two~~into collected ~~141~~ clay infilling samples within two main cave systems: the *Grotte-Exurgence du Garrel*  
184 and the *Aven de la Leicasse* (Fig. 1). These two sites-cave systems allowed us collecting samples along a more  
185 continuous range of elevations than the one provided by the Rieutord samples (for burial age determination) and  
186 also ~~allowed~~ extending the spatial coverage to the Southern Grands Causses region. Thanks to the geometry of  
187 these two cave systems, we sampled a 400m downward base level variation. The sampling was done along verti-

188 | cal profiles from a few ten of centimeters to 2 meters high by means of Plexiglas cubes with a 2 cm edge length  
189 (Fig. 4) used as a pastry cutter. We weren't able to analyse clay samples from Rieutord canyon because no reli-  
190 able clay infilling was found in the Rieutord caves.

191 Demagnetisation was performed with an applied alternative field up to 150mT using a 2G-760 cryogenic mag-  
192 netometer, equipped with the 2G-600 degausser system controller. Before this analysis, each sample remained at  
193 least 48h in a null magnetic field, preventing a possible low coercivity viscosity overprinting the detrital rema-  
194 nent magnetisation (DRM) (Hill, 1999; Stock et al., 2005; Hajna et al., 2010). If the hypothesis of instantaneous  
195 locked in DRM seems reasonable compared with the studied time span, it is important to keep in mind that the  
196 details of DRM processes (as for instance the locked in time) is not well understood (Tauxe et al., 2006; Spassov  
197 et Valet, 2012) and could possibly lead to small variations (few percents) in the following computed incision  
198 rates.

199 Because fine clay particles are expected being easily reworked in the cave, careful attention was paid to the site  
200 selection and current active galleries were avoided. Clays deposits had to show well laminated and horizontal  
201 layering in order to prevent analysis of in-situ produced clays (from decalcification) or downward drainage by  
202 an underneath diversion gallery that could strongly affect the obtained inclination (and also the declination to a  
203 minor extent). Note that for paleo-polarities study alone, small inclination or declination variations won't result  
204 in false polarities

## 205 **2.2 Quantifying the average incision rates**

### 206 **2.2.1. Rieutord incision rate from burial ages**

207 | The relationship between burial ages and incision is shown in Figure 5. ~~Except for the Camp-de-Guerre~~  
208 ~~cave (CDG) site, the higher the cave is, the older the burial ages are. For the four caves, we observed a good re-~~  
209 ~~lationship between burial ages and finite incision, except for the Camp-de-Guerre cave (CDG) site, the higher~~  
210 ~~the cave is, the older the burial ages are. Burial ages for the Cuillère cave, Dugou cave, Camp-de-Guerre cave~~  
211 ~~and Route cave are  $2.16 \pm 0.15$ ,  $0.95 \pm 0.14$ ,  $0.63 \pm 0.1$  and  $0.21 \pm 0.1$  Myrs respectively.~~ This is consistent with  
212 the supposed cave evolution and first-order constant incision of the Rieutord canyon. CDG age has to be consid-  
213 ered with caution. The CDG cave entrance located in a usually dry thalweg can act as a sinkhole or an overflow-  
214 ing spring depending on the intensity of the rainfall. The sample was collected in a gallery showing evidence of  
215 active flooding ~10 m above the Rieutord riverbed, therefore the older than expected age, given the elevation of  
216 the cave, is probably due to cobbles that came from upper galleries during flood events. Forcing the linear re-  
217 gression to go through the origin, leads to an incision rate of  ~~$832.8 \pm 354.9$~~   $m.Ma^{-1}$ . These results show that at  
218 least half of the 300 m deep Rieutord Canyon is a Quaternary incision. Extrapolating the obtained rate yields an  
219 age of  $4.4 \pm 1.9$  Ma for the beginning of the canyon incision, which suggests that the current landscape has been  
220 shaped during the Plio-Quaternary period. To extend our spatial coverage and bring stronger confidence into our  
221 results, we combine Rieutord burial ages with paleomagnetic data from watersheds located on the other side of  
222 the Herault watershed.

### 223 **2.2.2. South Grands Causses incision rate from paleomagnetic data**

224 | A total of 1004+ clay-infilling samples distributed over of 13 sites (i.e. profiles) were he~~Of the two cave sys-~~  
225 ~~tems, +studied.~~ The lowest sample elevation above sea level (a.s.l.) is in the Garrel (ca 190 m) and the highest in

226 the Leicasse (ca 580 m a.s.l.). ~~Given the very marginal difference in elevation between the local base levels~~  
227 ~~from these two caves, we assume that they have the same local base level reference.~~ In the Leicasse cave sys-  
228 tem, we sampled 8 ~~profiles for a total sites totalizing of 60+~~ samples. ~~Their Profiles~~ elevations are located be-  
229 tween ca 200 m and ca 400 m above ~~the~~ base level (a.b.l.), ~~which corresponds defined as to~~ the elevation of the  
230 Buèges river spring at 170 m ~~above sea level~~ a.s.l.

231 ~~In the Garrel cave system, we sampled From 5 sites profiles totalizing, the 480 Garrel samples that encompass~~  
232 ~~elevations range between 20 m and 80 m a.b.l. defined by the Garrel spring at 180 m a.s.l. Given the very mar-~~  
233 ~~marginal difference in elevation between the local base levels from these two caves, we assume that they have the~~  
234 ~~same local base level. At each studied sites, if all the profile samples have the same polarity, the site is granted~~  
235 ~~with the same polarity, either normal or reverse. If not (i.e. the profile displays normal and reverse polarities),~~  
236 ~~we consider it as a transitional site. Figure 6 shows the results plotted with respect to the paleomagnetic scale (x~~  
237 ~~axis) for the past 7 Ma, and their elevation above the base level (y axis). The measured paleomagnetic polarities~~  
238 ~~on each sites is plotted several times for given incision rates supposed to be constant through times (this allows~~  
239 ~~determining different age models and analyze their correlation with the distribution of paleomagnetic data, see~~  
240 ~~below).~~

241 ~~by individual sites, in respect with their elevation a.b.l. If all the samples of one site have the same polarity, the~~  
242 ~~site is granted with the same polarity. If not, that is to say if the site displays normal and reverse polarities, we~~  
243 ~~consider it as a transitional site.~~

244 ~~for each 13the figure 6 represents the magnetic polarities can count between 3 to 15 samples (fig. 4), that on~~  
245 ~~site is a vertical profile of samples and each~~ Because

246 ~~First, we note a good agreement between samples located at the same elevation~~ elevation and being part of the  
247 same stratigraphic layer (Camus, 2003). This syngenetic deposition allow, as best explanation to, prevent~~ing~~  
248 ~~from a possible partial endokarstic reworking. Second, the different elevations of the galleries where we collect-~~  
249 ~~ed the samples allow us to proposinge that the Leicasse and the Garrel deposits encompass at least three~~ chrons,  
250 while the Garrel deposits encompass and one only one polarity chrons, respectively. Third, Furthermore, a transi-  
251 tional signal comprised between a reversal signal (lower samples) and a normal signal (upper ones) is observed  
252 at Les Gours sur Pattes (LGP) sampling site ~~normal being "reverse", the upper ones "lower samples, the a re-~~  
253 ~~versal signal record transitional signal and the sample in between show a~~ (Fig. 7). This specific site provides a  
254 strong constraints on the age of the sediment emplacement in the Leicasse with respect to ~~in~~ the magnetostrati-  
255 graphic timescale (Fig. 6).

256 Compared to the Leicasse cave system, the elevation/polarity results for the Garrel are less constrained. Only  
257 Although poorly constrained since it relies on a single one sample site with shows a reverse polarity at (90 m  
258 a.b.l.), and the transitional polarity found at 40 m a.b.l. is unclear (tab, suppl mat.). The rest of the polarities (72  
259 samples) are all normal. Given that a agrees with elevation/polarity results for the Garrel the, U-Th ages  
260 younger than 90 kyrs was obtained for two speleothems (Camus, 2003) that covering our samples delays col-  
261 lected in the Garrel at ca 40 m a.b.l. (Camus, 2003) (Fig. 6), speleothems despite 72 collected samples, the re-  
262 versed polarities have been found beneath clear. Since no we assume consider that the emplacement of these the  
263 clays deposits occurred during the most recent normal period and are therefore younger than 0.78 Ma (Figure  
264 6). The transition between the highest normal sample and the reversed one is located somewhere between 78 m  
265 and 93 m a.b.l. suggesting a maximum base level lowering rate of  $109.6 \pm 9 \text{ m.Ma}^{-1}$  ~~sample with probable reverse polarity but poor~~

266 ~~quality b.l. is so only because of one a Mat ca. 40 and located as reversal signal ed. Note that the site display.~~

267 To go further in the interpretation of our data, and better constraint the incision rate, we analyzed performed a  
268 correlation analysis various incision rates the between observed and modelled polarities for a 0 - 200 m.Ma-1  
269 incision-rate range (linear rate, each 1m.Ma-1). Modelled polarities are found and computed a correlation fac-  
270 tor based on the consistency between the observed polarities and the modelled ones, for each sample related to  
271 the previously computed age, from both the Garrel and the Leicasse cave systems, as a function of various inci-  
272 ision rates ranging from 0 to 200 m.Ma<sup>-1</sup> with a 1 m.Ma<sup>-1</sup> step.

273 Then, from the magnetostratigraphic timescale, we extracted the theoretical polarity for every clay sample, we  
274 computed theoretical age models position of the sample a.b.l. knowing the us from studying possible variations  
275 of the incision rate through time. Given our results for the Rieutord samples we assume that the incision rate can  
276 be considered to the first order as linear through time.

277 Therefore, s sampling resolution prevent our the Unfortunately

278 ay block or an excursion signal can be explain for instance by a local remobilization of a ethe Matuyama peri-  
279 od we prefer not to give a strong weigh to this unique sample thatre, if we can propose it as being part of There-  
280 fo

281 using the intersection between sample elevation and incision-rate line.

282 We obtained 10 possible incision rates with the same best correlation factor (Fig. 8) spanning from 43 to 111  
283 m.Ma<sup>-1</sup> (mean of  $87.2 \pm 243.8$  m.Ma<sup>-1</sup>). Taking into account the transitional signal of the LGP site in the Leicas-  
284 se cave yields a linear incision rate of  $83.4^{+17.3}/_{-5.4}$  m.Ma<sup>-1</sup>. Proposed uncertainties are based on previous and next  
285 transition-related estimated incision rate.

286 Using a similar approach for the Rieutord crystalline samples, that is to say we compute, for the same inci-  
287 ision-rate space, the distance in a least square sens between the modeled age and the measured ones in order to  
288 check the cost function shape and acuteness. With this method, we determined a linear incision rate of  $85 \pm 11$   
289 m.Ma<sup>-1</sup> (Fig 8). Those two results, based on independent computations, suggest the same first-order incision rate  
290 for the last 4 Ma of  $84.2^{+219.5}/_{-12.3}$  m.Ma<sup>-1</sup>. Given that the Rieutord, Garrel and Buèges rivers are all tributaries of  
291 the Hérault river, we propose that this rate represents the incision rate for the Hérault river watershed, inducing  
292 approximately 300-350 m of finite incision over the Plio-Quaternary period.

293 If the landscape is at first order in an equilibrium state, that is to say, if we preclude our incision rates being a re-  
294 gressive erosional signal, the incision needs to be balanced by an equivalent amount of uplift. If the uplift rate is  
295 roughly correlated to the regional topography, lowest uplift rates would be expected in the south of our sampling  
296 sites inducing regional tilting of morphological benchmarks. In the next part, we search for such evidences that  
297 would suggest differential uplift.

### 298 2.3 Geomorphometrical **evidene**approach

299 According to the Massif-Central centered uplift hypothesis, morphological markers such as strath terraces, flu-  
300 vio-karstic surfaces or abandoned meanders should display a southward tilting due to differential uplift between  
301 the northern and the southern part of the region, with the expected following signals:

302 The dipping direction of the tilted markers should be parallel to the main gradient of the topography, i.e. be-  
303 tween 150°E and 180°E for our studied region. This expectation is the most important one, regarding uncertain-  
304 ties on the uplift rate and lithospheric elastic parameters.

305 ~~—A latitudinal tilting trend, i.e. an increase of the tilt angle along the topography gradient. Indeed, null or small~~  
306 ~~tilts are expected near the shoreline and within the maximum uplift area of the Cevennes/Massif Central, while~~  
307 ~~the maximum tilt is expected at a mid distance between these two regions, i.e. about 50 km inland from the~~  
308 ~~shoreline.~~

309 ~~—A positive altitudinal tilting trend (an increase in dip angle with altitude). This trend would be representative~~  
310 ~~of the accumulation of finite tilt. However, it supposes a linear relationship between the altitude and the age of~~  
311 ~~the marker formation. If at first order, this straightforward hypothesis seems reasonable for river-controlled~~  
312 ~~markers (e.g. strath terraces), other surfaces are hardly expected to follow such an easy relationship.~~

313 \_\_\_\_\_ To investigate these different signals, we used the morphological markers available for the study area  
314 (Fig. 9). We used a 5 m resolution DEM analysis to identify the markers corresponding to surfaces with slope <  
315 2°. This cut-off slope angle prevents to identify surface related to local deformation such as for example land-  
316 slide or sinkhole. Other issue could be due to diffusion processes that could create apparent tilting. However that  
317 problem is adress by 1) the automatic selection and correction and the final manual check for residue random  
318 distribution (see below).—The local river slope is on the order of 0.1° so the 2° cut-off angle is far from preclud-  
319 ing to identify tilted markers. We also us a criterion based on an altitudinal range for a surface. This altitudinal  
320 span is set individually for each surface based on elevation, slope and curves map analysis, and encompass from  
321 few meters to tens of meters depending on the size of the marker. We checked 80% of the identified surfaces in  
322 the field in order to avoid misinterpretation. Some pictures are provided in supplementary material. The dip di-  
323 rection and angle of the surface in computed in a two steps approach. First, we compute fit a plan using extracted  
324 points from the DEM inside the delimited surface. Second, based on this plan we remove the DEM points with  
325 residuals 3 times larger than the standard error and compute more accurate plan parameters (second fitting).  
326 This outlier suppression removes any inaccurate DEM points and correct for inaccurate surface delimitation  
327 (e.g. integration of a part of the edge of a strath terrace, diffusion processes marks, etc.).

328 Because no obvious initially horizontal markers are known, we propose to correct the marker current slope by  
329 the initial one to quantify the tilt since the marker emplacement. To do so we follow the method used by Cham-  
330 pagnac et al. (2008) for the Forealps. We identify the drain related to the marker formation and compute its cur-  
331 rent local slope and direction. This method assumes that landscapes are at the equilibrium state and that the river  
332 slope remained constant since the marker formation. This assumption seems reasonable given the major river  
333 profiles and because most of the markers used are far from the watershed high altitude areas precluding a reces-  
334 sive erosional signal. Finally, we removed the local river plan from the DEM extracted surface.

335 Following this methodology, we obtained 61 surfaces. We then applied three quality criterions to ensure the ro-  
336 bustness of our results: 1) The minimal surface considered is 2500 m<sup>2</sup> based on a comparison between the 5m  
337 resolution DEM and a RTK GPS survey over 3 strath terraces (Hérault river); 2) Final plans with dip angles  
338 larger than 2° are removed; 3) The residuals for each geomorphological marker must be randomly distributed  
339 without marker edge signal, or clear secondary structuration. Only 38 markers meet those 3 quality criterions.

340 If the identified and corrected markers had indeed registered an differential uplift between the north and the  
341 south, we expected the following signals:

342 - The dipping direction of the tilted markers should be parallel to the main gradient of the topography, i.e. be-  
343 tween 150°E and 180°E for our studied region. This expectation is the most important one, regarding uncertain-

344 | ties on the uplift rate and lithospheric elastic parameters.

345 | - A latitudinal tilting trend, i.e. an increase of the tilt angle along the topography gradient. Indeed, null or small  
346 | tilts are expected near the shoreline and within the maximum uplift area of the Cevennes/Massif Central, while  
347 | the maximum tilt is expected at a mid-distance between these two regions, i.e. about 50 km inland from the  
348 | shoreline.

349 | - A positive altitudinal tilting trend (an increase in dip angle with altitude). This trend would be representative  
350 | of the accumulation of finite tilt. However, it supposes a linear relationship between the altitude and the age of  
351 | the marker formation. If at first order, this straightforward hypothesis seems reasonable for river-controlled  
352 | markers (e.g. strath terraces), other surfaces are hardly expected to follow such an easy relationship.

353 | Among the three expected signal, southward dipping is robustly recorded with~~The results show~~ a mean tilt an-  
354 | gle of  $0.60 \pm 0.40$  ° with an azimuth of N12850 ± 3640°E (Fig. 10). Latitudinal trend and altitudinal trend are  
355 | less robustly reached but that is not surprising because of the strong susceptibility to local phenomenon or even  
356 | so lack of robust age constraint.

### 357 | **3 Numerical modelling**

358 | Both geomorphological and geochronological evidence suggest a Plio-Quaternary uplift of the Cevennes area.  
359 | The origin of such uplift could be associated with several processes: erosion-induced isostatic rebound, dynamic  
360 | topography due to mantle convection, thermal isostasy, residual flexural response due to the Gulf of Lion forma-  
361 | tion, etc. For the Alps and Pyrenees mountains, isostatic adjustment due to erosion and glacial unloading has  
362 | been recently quantified (Champagnac et al., 2007, Vernant et al., 2013; Genti et al, 2016, Chery et al. 2016).  
363 | Because the erosion rates measured in the Cevennes are similar to those of the Eastern Pyrenees (Calvet et al.,  
364 | 2015, Sartégou et al., 2018a), we investigate by numerical modelling how an erosion-induced isostatic rebound  
365 | could impact the southern Massif Central morphology and deformation.

366 | We define a representative cross-section parallel to the main topographic gradient (i.e. NNW-SSE) and close to  
367 | the field investigation areas (Figure 11). We study the lithospheric elastic response to erosion with the 2D finite  
368 | element model ADELI (Hassani et Chery, 1996; Chéry et al. 2016). The model is composed of a plate account-  
369 | ing for the elasticity of both crust and uppermost mantle. Although the lithosphere rigidity of the European plate  
370 | in southern Massif central is not precisely known, vertical gradient temperatures provided by borehole measure-  
371 | ments are consistent with heat flow values ranging from 60 to 70 mW.m<sup>2</sup> (Lucazeau et Vasseur, 1989). There-  
372 | fore, we investigate plate thickness ranging from 10 to 50 km as done by Stewart et Watts (1997) for studying  
373 | the vertical motion of the alpine forelands. We choose values for Young's and Poisson parameters of respective-  
374 | ly 10<sup>11</sup> Pa and 0.25, both commonly used values for lithospheric modelling (e.g. Kooi et Cloething, 1992;  
375 | Champagnac et al. 2007, Chéry et al., 2001). This leads to long-term rigidity of the lithosphere model ranging  
376 | from 10<sup>21</sup> to 10<sup>25</sup> N.m. Since the effect of mantle viscosity on elastic rebound is assumed to be negligible at the  
377 | time scale of our models (1 to 2 Myrs), we neglect the visco-elastic behaviour of the mantle. Therefore, the base  
378 | of the model is supported by an hydrostatic pressure boundary condition balancing the weight of the lithosphere  
379 | (Fig. 11). Horizontal displacements on vertical sides are set to zero since geodetic measurements show no sig-  
380 | nificant displacements (Nocquet et Calais, 2003; Nguyen et al., 2016). The main parameters controlling our

381 model are the erosion (or sedimentation) triggering isostatic rebound and the elastic thickness. The erosion pro-  
382 file (Fig. 11) is based on topography, our newly proposed incision rate and other studies (Olivetti et al., 2016 for  
383 onshore denudation and Lofi et al., 2003; Leroux et al., 2014 for offshore sedimentation). This profile is a sim-  
384 plification of the one that can be expected from Olivetti et al. (2006) and do not aim at matching precisely the  
385 published data because of, first, the explored time-span (~ 1 Myrs) is not covered by thermochronological data  
386 (> 10Myrs) or cosmogenic denudation rate (10s-100s kyrs). Second, we base our erosion rate as being linked  
387 with local (10s km<sup>2</sup>) slopes, that are higher near the drainage divide. We, by this aim can invoke any kind of ero-  
388 sion processes (e.g. landslides). Third, the model suppose a cylindrical structure and then, high-frequency later-  
389 al variations in term or actual denudation rate or proxy (slope, elevation, etc.) must be averaged. Concerning this  
390 erosion profile, parametric study (highest erosion rate ranging from 1 to 1000 m.Myrs<sup>-1</sup>) give no difference in  
391 the interpretation and, for few percent variations, only few percent variations in the modeled uplift-rate.

392 \_\_\_\_\_ The flexural rigidity controls the intensity and wavelength of the flexural response and ranges from 10<sup>21</sup>  
393 to 10<sup>25</sup> N.m. It can be expressed as a variation in elastic thickness (Te) ranging from 4.4 to 96 km (Fig. 12). We  
394 also test a possible Te variation between inland and offshore areas. For the following discussion, we use an elas-  
395 tic thickness of 15km corresponding to a value of D of 3.75 x10<sup>23</sup> N.m<sup>-1</sup>. In this case, the inland and offshore  
396 parts are largely decoupled and the large sedimentation rate in the Gulf of Lion does not induce a flexural re-  
397 sponse on the Cévennes and Grands Causses areas. With a maximum erosion rate of 80 m.Ma<sup>-1</sup> (Fig 11), the  
398 models display uplift rates of 50 m.Ma<sup>-1</sup> over more than 100 km. As previously explained, the finite incision is  
399 permitted by an equal amount of uplift considering that the incision is not due to regressive erosion. If all tested  
400 models show uplift, the modelled amplitudes are smaller than the expected ones. To obtain the same uplift rate  
401 than the incision rates, the applied erosion rate over the model must be increased. However, we assume that the  
402 landscape is at equilibrium, so, if the erosion rate is increased, it will be higher than the incision rate leading to  
403 the decay of relief over the area. No evidence of such evolution is found over the region and, if further studies  
404 need to be done to quantify the actual erosion rate, we mostly think that a second process is acting, inducing the  
405 rest of the uplift that can't be obtained by the erosion-induced isostatic adjustment. Finally, models predict a  
406 seaward tilt of the surface at the regional-scale (Fig. 13), in agreement with the observed tilting of morphologi-  
407 cal markers.

#### 408 4. Discussion

409 We assume that the sediments collected in the karst were deposited per descensum, i.e. we do not know  
410 if the galleries existed a long time before or were formed just before the emplacement of the sediments, but the  
411 more elevated the sediments are, the older their deposit is. If there is no evidence of an important aggradation  
412 episode leading to more a complex evolution as proposed for the Ardèche canyon (Moccochain et al., 2007;  
413 Tassy et al., 2013), we point out that small aggradation or null erosion period could, however, be possible. Some  
414 processes could explain such relative stability: e.g. variation in erosion (due to climatic fluctuation) or impact of  
415 eustatic variations (in river profile, flexural response, etc.). Such transient variations have been shown for the  
416 Alps (Saillard et al., 2014; Rolland et al., 2017) and are proposed as being related to climato-eustatic variations  
417 and therefore should last 10 to 100 kyrs at most.

418 Based on our sampling resolution, we cannot evidence such transient periods and we must use an average base  
419 level lowering rate in the karst, which we correlate to the incision of the main rivers. The TCN-based incision

420 | rate derived from the Rieutord samples ( $832.8 \pm 354.9$  m.Ma<sup>-1</sup>) is consistent with the one derived from the Gar-  
421 | rel (U-Th ages: 85.83 m.Ma<sup>-1</sup> according to the sole U/Th exploitable result (Camus, 2003)) and from the Garrel-  
422 | Leicasse combination (Paleomagnetic approach:  $84.2^{+210.5}_{-123}$  m.Ma<sup>-1</sup>).

423 | This mean incision rate of ca. 85 m.Ma<sup>-1</sup> lasting at least 4 Ma, highlights the importance of the Plio-Quaternary  
424 | period into the Cévennes and Grand Causses morphogenesis. Furthermore, the 300 to 400 m of incision pre-  
425 | cludes a relative base level controlled by a sea-level drop. Indeed, documented sea level variations are less than  
426 | 100 m (Haq, 1988, Miller et al., 2005). Furthermore, the Hérault river does not show any significant knickpoints  
427 | or evidence of unsteadiness in its profile as expected if the incision was due to eustatic variations. Therefore, we  
428 | propose that the incision rate of ~85 m.Ma<sup>-1</sup> is due to a plio-quaternary uplift of the Cévennes and Grands  
429 | Causses region.

430 | Other river-valley processes could lead to a local apparent high incision rate as for instance major land-  
431 | slide or alluvial fan (Ouimet et al., 2008). This hypothesis of an epigenetic formation of the Rieutord is irrele-  
432 | vant because of i) none of the possible causes had been found in the Rieutord canyon and ii) the consistency of  
433 | the TCN-based incision rate and the paleomagnetic-based incision rate for two other cave-systems. Indeed, the  
434 | use of two independent approaches and three locations is a good argument in favour of the robustness of our  
435 | proposed mean 85 m.Ma<sup>-1</sup> incision rate. Yet, using more data, particularly burial dating colocalized with clays  
436 | samples and adding sampling sites would give a stronger statistical validation. In the Lodève basin (Point 4, fig.  
437 | 1), inverted reliefs allow another independent way to quantify minimal incision rate. K/Ar and paleomagnetic  
438 | dated basaltic flows spanning from 1 to 2 Myrs old that were deposited at the bottom of the former valley (Dau-  
439 | tria et al., 2010) are now located at ca 150 m above the current riverbed leading to an average incision rate of  
440 |  $776.5 \pm 10$  m.Myr<sup>-1</sup>, in agreement with karst-inferred incision rates.

441 | Furthermore, preliminary results from canyons on the other side of the Grands Causses (Tarn and Jonte) based  
442 | on in-situ terrestrial cosmogenic dating suggest similar incision rates (Sartegou et al., 2018b) and confirm a re-  
443 | gional base level lowering of the Cévennes and Grands Causses region during the Plio-Quaternary. This is con-  
444 | sistent with the similarities of landscapes and lithologies observed both on the Atlantic and Mediterranean wa-  
445 | tersheds (e.g. Tarn river).

446 | Once the regional pattern of the Plio-Quaternary incision established for the Cévennes-Grands Causses  
447 | area, the next question is how this river downcutting is related to the regional uplift? First order equilibrium  
448 | shape and absence of major knick points in the main river profiles preclude the hypothesis of regressive erosion.  
449 | Hence, back to the three conceptual models presented in part 1 (Fig 2), we can discard, at first order, the models  
450 | A (Old uplift-recent incision) and B (Old uplift-old incision) because obtain incision rate show recent incision  
451 | and surface tilting tend to prove a current uplift. Therefore, the incision rate has to be balanced to the first order  
452 | by the uplift rate. We add that eustatic variations are of too low magnitude (100-120 m) and can't explain such  
453 | total incision (up to 400m). Furthermore, nNo obvious evidence of active tectonic is reported for the area raising  
454 | the question of the processes responsible for this regional uplift. Very few denudation rates are reported for our  
455 | study area (Schaller et al., 2001; Molliex et al., 2016; Olivetti et al., 2017), and converting canyon incision rates  
456 | into denudation and erosion rates is not straightforward, especially given the large karst developed in the area.  
457 | Using a first order erosion/sedimentation profile following the main topography gradient direction we have  
458 | modelled the erosion-induced isostatic rebound. If this process could create between half and two third of the  
459 | Plio-Quaternary uplift, a previously existent topography is needed to trigger erosion so it cannot explain neither

460 the onset of the canyon-carving nor the full uplift rates. Other, processes have to be explored such as dynamic  
461 topography or thermal anomaly beneath the Massif-Central, the magmatism responsible for the important in-  
462 crease in volcanic activity since ~ 6 Myrs (Michon et Merle, 2001; Nehlig et al., 2003) could play a major role,  
463 notably in the initiation of Plio-Quaternary uplift. [Further studies should aim to address the problem of uplift on-](#)  
464 [set, giving more clues concerning the stable continental area but owing the data we presently have, discussing](#)  
465 [such onset is out of the scope of the paper.](#)

## 466 5. Conclusion

467 To the contrary of previous studies that focused on one cave, we have shown that combining karst buri-  
468 al ages and paleomagnetic analysis of clay deposits in several caves over a large elevation range can bring good  
469 constraints on incision rates. This multi-cave system approach diminishes the intrinsic limits of the two single  
470 methods: low sampling density (and analysis cost) for the TCN ages and difficulty to set the position of paleo-  
471 magnetic results. Our estimated paleo base level ages are Plio-Quaternary (ca. last 4 Ma) and allow to derive a  
472 mean incision rate of  $83.4^{+17.3}/_{-5.4}$  m.Ma<sup>-1</sup> for the Cévennes area.

473 The landscape, and especially the river profiles suggest a first-order equilibrium allowing considering  
474 the incision rate as an uplift rate. We propose that related erosional isostatic adjustment is of major importance  
475 for the understanding of the southern French Massif-Central landscape evolution and explain a large part of the  
476 uplift. However, it is not the only process involved and we hypothesize that it could be especially combined  
477 with dynamic topography related to the Massif Central magmatism. Both mechanisms imply an uplift centered  
478 on the Massif Central and a radial tilt of the geomorphological surfaces. We have shown using a geomorpholog-  
479 ical analysis that at least south of the Cévennes, several surfaces are tilted toward the SSE. This kind of study  
480 had been performed before on large structures (Champagnac et al., 2007) or endokarstic markers (Granger et  
481 Stock, 2004) but it is the first time that it is performed at such scale with small markers. Numerical modelling  
482 yields the same pattern of SSE dipping, allowing more confidence in the geomorphometric results.

483 Our multi-disciplinary approach brings the first absolute dating of the Cévennes landscapes and suggests that the  
484 present-day morphology is partly inherited from the plio-quaternary erosion-induced isostatic rebound. A strong  
485 uplift impact is assumed to be due to magmatic-related dynamic topography that could explain another part of  
486 the uplift as well as the onset of such uplift that has afterward been accelerated by the erosion-induced isostatic  
487 rebound. These results enlighten the importance of surface processes into lithospheric-scale dynamic and verti-  
488 cal deformations in intra-plate domains.

489 An analysis at the scale of the Massif Central is now needed before nailing down our interpretations,  
490 but such study will more likely highlight the importance of erosion processes to explain uplift of intraplate oro-  
491 gens, and will show that another process is needed for the Massif Central, which will most likely be dynamic to-  
492 pography related to magmatism.

### 493 [Code availability](#)

494 [Surface analysis was performed using QGIS version 2.18, Matlab® code and IGN DEM \(RGE Alti®\) 5m.](#)  
495 [Modeling was performed using ADELI code \(Hassani et Chery, 1996; Chéry et al., 2016\). Data for TCN and](#)  
496 [paleomagnetic analysis are provided in the manuscript itself or in supplementary material.](#)

497 **Author contributions**

498 OM, PV and GC did the sampling. GC and DF performed the TCN analysis. PC and OM did the magnetic  
499 measurements and interpretations. OM did the surface identification and analysis. OM, PV and JC performed  
500 the numerical model. OM, OV, JFR, GC, PC, JC and DF interpreted and wrote the article.

501 **Competing interests**

502 The authors declare that they have no conflict of interest.

503 **Acknowledgments**

504 We are grateful to ANSTO for providing facilities for chemical extraction for the TCN analysis. We thanks the  
505 reviewers for useful remarks and comments that we think help to increase the level of the paper.

506 **References**

507 Arthaud F. et Laurent P.: Contraintes, déformations et déplacements dans l'avant-pays pyrénéen du Languedoc  
508 méditerranéen, *Geodin. Acta*, 8, 142-157, 1995.

509 Audra P., Camus H. et Rochette P.: Le karst des plateaux de la moyenne vallée de l'Ardèche : datation par  
510 paléomagnétisme des phases d'évolution plio-quaternaires (aven de la Combe Rajeau). *Bull. Soc. Géol. France*,  
511 2001, t. 172. N°1, pp. 121-129, 2001.

512 Balco, G., Stone, J.O., Lifton, N.A., Dunai, T.J., 2008. A complete and easily accessible means of calculating  
513 surface exposure ages or erosion rates from Be-10 and Al-26 measurements. *Quat. Geochronol.* 3, 174–195.  
514 2008.

515 Barbarand J., Lucazeau F., Pagel M. Et Séranne M.: Burial and exhumation history of the south-eastern Massif  
516 Central (France) constrained by apatite fission-track thermochronology. *Tectonophysics*, 335, 275-290, 2001.

517 Barruol G. et Granet M.: A Tertiary asthenospheric flow beneath the southern French Massif Central indicated by  
518 upper mantle seismic anisotropy and related to the west Mediterranean extension. *Earth and Planetary Science*  
519 *Letters* 202 (2002) 31-47, 2002.

520 Brichau S., Respaut J.P. et Monié P.: New age constraints on emplacement of the Cévenol granitoids, South  
521 French Massif Central, *Int J Earth Sci* 97:725–738, doi: 10.1007/s00531-007-0187-x, 2007.

522 Bruxelles L.: Dépôts et altérites des plateaux du Larzac central : causes de l'Hospitalet et de Campestre  
523 (Aveyron, Gard, Hérault) Evolution morphogénétique, conséquences géologiques et implications pour  
524 l'aménagement. Université d'Aix-Marseille I, Université de Provence, UFR Sciences géographiques et de  
525 l'aménagement. Thèse, spécialité : Milieux physiques méditerranéens, 2001.

526 Calais, E., Freed, A. M., Van Arsdale, R., & Stein, S. (2010). Triggering of New Madrid seismicity by late-  
527 Pleistocene erosion. *Nature*, 466(7306), 608–611. <http://doi.org/10.1038/nature09258>

528 Calais, E., T. Camelbeeck, S. Stein, M. Liu, and T. J. Craig (2016), A new paradigm for large earthquakes in  
529 stable continental plate interiors, *Geophys. Res. Lett.*, 43, doi:10.1002/2016GL070815, 2016.

530 Calvet M., Gunnell Y., Braucher R., Hez G., Bourlès D., Guillou V., Delmas M. et ASTER team: Cave levels as  
531 proxies for measuring post-orogenic uplift : Evidence from cosmogenic dating of alluvium-filled caves in the  
532 French Pyrenees. *Geomorphology* 246 (2015) 617- 633 ; doi : 10.1016/j.geomorph.2015.07.013, 2015.

533 Camus H.: Vallée et réseaux karstiques de la bordure carbonatée sud-cévenole. Relation avec la surrection, le  
534 volcanisme et les paléoclimats. Thèse de doctorat, Université Bordeaux 3, 692 p, 2003.

535 Champagnac J.D., Molnar P., Anderson R.S., Sue C. et Delacou B.: Quaternary erosion-induced isostatic re-  
536 bound in the western Alps. *Geology*, March 2007 ; v.35 ; no. 3 ; p. 195-198, doi : 10.1130/G23053A.1, 2007.

537 Champagnac J-D. van der Beek P. Diraison G. et Dauphin S.: Flexural isostatic response of the Alps to in-  
538 creased Quaternary erosion recorded by foreland basin remnants, SE France. *Terra Nova*, Vol 20, No. 3, 213-  
539 220, doi : 10.1111/j.1365-3121.2008.00809.x, 2008.

540 Chéry J., Zoback M.D. et Hassani R.: An integrated mechanical model of the San Andreas Fault in central and  
541 northern California. *J. Geophys. Res.*, 106(B10) :22051. 52,61, 2001.

542 Chéry, J., Genti, M. And Vernant, P. Ice cap melting and low-viscosity crustal root explain the narrow geodetic  
543 uplift of the Western Alps. *Geophys. Res. Lett.* 43,1–8 (2016).

544 Child D.P., Elliott G., Mifsud C., Smith A.M and Fink D., Sample processing for earth science studies at  
545 ANTARES. *Nuclear Instruments and Methods in Physics Research Section B Beam Interactions with Materials*  
546 *and Atoms* 172(1-4):856-860 doi: 10.1016/S0168-583X(00)00198-1, 2000.

547 Corbel J.: Les phénomènes karstiques dans les Grands Causses. In : *Revue de géographie de Lyon*, vol. 29, n°4,  
548 pp. 287-315, doi : 10.3406/geoca.1954.1990, 1954.

549 Dautria J.M., Liotard J.M., Bosch D., Alard O.: 160 Ma of sporadic basaltic activity on the Languedoc volcanic  
550 line (Southern France): A peculiar cas of lithosphere-asthenosphere interplay. *Lithos* 120 (2010) 202-222, doi:  
551 10.1016/j.lithos.2010.04.009, 2010

552 Genti M.: Impact des processus de surface sur la déformation actuelle des Pyrénées et des Alpes. *Géophysique*  
553 [physics.geo-ph]. Université de Montpellier, 2015. Français. Thèse, 2016.

554 Granet M., Wilson M. et Achauer U.: Imaging a mantle plume beneath the French Massif Central. *Earth and*  
555 *Planetary Science Letters* 136 (1995) 281-296, 1995.

556 [Granger, D. E., Fabel, D. and Palmer, A.N.: Pliocene-Pleistocene incision of the Green River, Kentucky deter-](#)  
557 [mined from radioactive decay of comogenic 26Al and 10Be in Mammoth Cave sediments. \*GSA Bulletin\*; July](#)  
558 [2001; v. 113; no. 7; p. 825–836](#)

559 Granger, D. E., Kirchner, J. W., ~~and~~ Finkel, R. C.: Quaternary downcutting rate of the New River, Virginia,  
560 measured from differential decay of cosmogenic 26Al and 10Be in cave-deposited alluvium. *Geology*; Febru-  
561 rary 1997 ; v. 25 ; no.2 ; p. 107-110, 1997.

562 Granger D.E., Gibbon R.J., Kuman K., Clarke R.J., Bruxelles L. ~~and~~ Caffee M.W.: New cosmogenic burial  
563 ages for Sterkfontein Member 2 Australopithecus and Member 5 Oldowan, *Nature Letter* 2015, doi:  
564 10.1038/nature14268, 2015.

565 Granger D.E. ~~and~~ Muzikar P.F.: Dating sediment burial with in situ-produced cosmogenic nuclides: theory,  
566 techniques, and limitations. *Earth and Planetary Science Letters* 188 (2001) 269-281, 2001.

567 | Granger D.E. ~~and~~ Stock G.M.: Using cave deposits as geologic tiltmeters : Application to postglacial rebound  
568 | of the Sierra Nevada, California. *Geophysical Research Letters*, vol. 31, L22501, doi : 10.1029/2004GL021403,  
569 | 2004.

570 | Zupan Hajna N., Mihevc A., Pruner P. ~~and~~ Bosák P. 2010. Palaeomagnetic research on karst sediments in  
571 | Slovenia. *International Journal of Speleology*, 39(2), 47-60. Bologna (Italy). ISSN 0392-6672, 2010.

572 | Haq B.U., Herdenbol J. ~~and~~ Vail P.R.: Mesozoic and cenozoic chronostratigraphy and cycles of sea-level  
573 | change. *Society Economic Paleontologists Mineralogists Special Publication*, 42, 71-108, Tulsa, Oklahoma.  
574 | 1988.

575 | Harmand D., Adamson K., Rixhon G., Jaillet S., Losson B., Devos A., Hez G., Calvet M. ~~and~~ Audra P.: Rela-  
576 | tionships between fluvial evolution and karstification related to climatic, tectonic and eustatic forcing in temper-  
577 | ate regions, *Quaternary Science Reviews* (2017) 1-19, doi : 10.1016/j.quascirev.2017.02.016, 2017.

578 | Hassani R. and Chery J., Anelasticity explains topography associated with Basin and Range normal faulting.  
579 | *Geology* 24(12):1095. doi: 10.1130/0091-7613(1996)024<1095:AETAWB>2.3.CO;2. 1996.

580 | Hill C.A., 1999.. Sedimentology and Paleomagnetism of sediments, Kartchner caverns, Arizona. *Journal of*  
581 | *Cave and Karst Studies* 61(2) : 79-83, 1999.

582 | Husson E.: Intéraction géodynamique/karstification et modélisation 3D des massifs carbonatés : Implication sur  
583 | la distribution prévisionnelle de la karstification. Exemple des paléokarsts crétacés à néogènes du Languedoc  
584 | montpelliérain. *Sciences de la Terre. Université Montpellier 2- Sciences et techniques du Languedoc*, 236 p,  
585 | 2014.

586 | Kooi H., Cloetingh S. et Burrus J.: Lithospheric Necking and Regional Isostasy at Extensional Basins 1. Subsidi-  
587 | dence and Gravity Modeling With an Application to the Gulf of Lions Margin (SE France), *Journal of Geophys-*  
588 | *ical Research* , vol. 97, no. B12, Pages 17,553- 17,571, november 10, 1992.

589 | Leroux E., Rabineau M., Aslanian D., Granjeon D., Droz L. et Gorini C.: Stratigraphic simulations of the shelf  
590 | of the Gulf of Lions: testing subsidence rates and sea-level curves during the Pliocene and Quaternary. *Terra*  
591 | *Nova*, Vol 26, No. 3, 230-238, doi: 10.1111/ter.12091, 2014.

592 | Lofi J., Rabineau M., Gorini C., Berne S., Clauzon G., De Clarens P., Dos Reis A.T., Mountain G.S., Ryan  
593 | W.B.F, Steckler M.S. et Fouchet C.: Plio-Quaternary prograding clinoform wedges of the western Gulf of Lion  
594 | continental margin (NW Mediterranean) after the Messinian Salinity Crisis., *Marine Geology* July 2003; 198 (3-  
595 | 4) : 289-317, doi: 10.1016/S0025-3227(03)00120-8, 2003.

596 | Lucazeau F. and Vasseur G.: Heat flow density data from France and surrounding margins, In: V. Cermak, L.  
597 | Rybach and E.R. Decker (Editors), *Tectonophysics*, 164 (1989) 251-258

598 | Manchuel K., Traversa P., Baumont D., Cara M., Nayman E. Et Durouchoux C.: The French seismic CATa-  
599 | logue (FCAT-17), *Bull Earthquake Eng* (2018) 16:2227–2251, doi: 10.1007/s10518-017-0236-1, 2018.

600 | Miallier D., Michon L., Evin J., Pilleyre T., Sanzelle S., et Vernet G.: Volcans de la Chaîne des Puys (Massif  
601 | Central, France) : point sur la chronologie Vasset-Kilian-Pariou-Chopine. *Comptes Rendus Géoscience*, Elsevier  
602 |

603 | Michon L. et Merle O.: The evolution of the Massif Central rift: Spatio-temporal distribution of the volcanism.  
604 | *Bulletin de la Society Geologique de France*, 2001, t. 172, n°2, pp. 201-211, doi: 10.1130/172.2.201, 2001.

605 | Miller, K.G., Kominz, M.A., Browning, J.V., Wright, J.D., Mountain, G.S., Katz, M.E., Sugarman, P.J., Cramer,  
606 | B.S., Christie-Blick, N., Pekar, S.F.: The Phanerozoic record of global sea-level change. *Science* 310, 1293–  
607 | 1298, doi : 10.1126/science.1116412, 2005.

608 Mocochain L.: Les manifestations géodynamiques –Externes et internes- de la crise de salinité messinienne sur  
609 une plate-forme carbonatée peri-méditerranéenne : le karst de la basse ardèche (moyenne vallée du Rhône ;  
610 France). Thèse de doctorat, Université Aix- Marseille I – Université de Provence U.F.R des Sciences  
611 géographiques et de l'aménagement Centre Européen de Recherches et d'Enseignement en Géosciences de  
612 l'Environnement., 196 p, 2007.

613 Molliex S., Rabineau M., Leroux E., Bourlès D.L., Authemayou C., Aslanian D., Chauvet F., Civet F. et Jouët  
614 G.: Multi-approach quantification of denudation rates in the Gulf of Lion source-to-sink system (SE-France).  
615 *Earth and Planetary Science Letters* 444 (2016) 101-115, doi : 10.1016/j.epsl.2016.03.043, 2016.

616 Nehlig P., Boivin P., de Goër A., Mergoïl J., Prouteau G., Sustrac G. Et Thiéblemont D.: Les volcans du Massif  
617 central. *Revue BRGM: Géologues, Numéro Spécial: Massif central*, 2003.

618 Nguyen H. N., Vernant P., Mazzotti S., Khazaradze G. et Asensio E.: 3-D GPS velocity field and its implica-  
619 tions on the present-day post-orogenic deformation of the Western Alps and Pyrenees. *Solid Earth*, 7 ; 1349-  
620 1363, 2016, doi : 10.5194/se-7-1349-2016, 2016.

621 Nocquet J.-M. et Calais E.: Crustal velocity field of western Europe from permanent GPS array solutions, 1996-  
622 2001. *Geophys. J. Int.* (2003) 154, 72-88, doi : 10.1046/j.1365-246X.2003.01935.x, 2003.

623 Nocquet J.-M., Sue C., Walpersdorf A., Tran T., Lenôtre N., Vernant P., Cushing M., Jouanne F., Masson F.,  
624 Baize S., Chéry J. and Van der Beek P.A., Present-day uplift of the western Alps, *Sci. Rep.* 6, 28404; doi:  
625 10.1038/srep28404 (2016).

626 Olivetti V., Godard V., Bellier O. et ASTER team : Cenozoic rejuvenation events of Massif Central topography  
627 (France) : Insights from cosmogenic denudation rates and river profiles. *Earth and Planetary Science Letters* 444  
628 (2016) 179-191, doi : 10.1016/j.epsl.2016.03.049 0012-821X, 2016.

629 Ouimet, WB, Whipple, KX, Crosby, BT, Johnson, JP, Schildgen, TF. 2008. Epigenetic gorges in fluvial land-  
630 scapes. *Earth Surface Processes and Landforms* 33: 1993– 2009. doi: 10.1002/esp.1650 Epigenetic. 2008.

631 Rolland Y., Petit C., Saillard M., Braucher R., Bourlès D., Darnault R. Cassol D. Et ASTER Team: Inner gorges  
632 incision history: A proxy for deglaciation? Insights from Cosmic Ray Exposure dating (10Be and 36Cl) of river-  
633 polished surfaces (Tinée River, SW Alps, France). *Earth and Planetary Science Letters*, Elsevier, 2017, 457,  
634 pp.271 - 281, doi : 10.1016/j.epsl.2016.10.007. <hal-01420882>, 2017.

635 Rovey II C.W., Balco G., Forir M. Et Kean W.F.: Stratigraphy, paleomagnetism, and cosmogenic-isotope burial  
636 ages of fossil-bearing strata within Riverbluff Cave, Greene County, Missouri. *Quaternary Research* (2017), 1-  
637 13, doi : 10.1017/qua.2017.14, 2017.

638 Saillard M., Petit C., Rolland Y., Braucher R., BOurlès D.L., Zerathe S., Revel M. Et Jourdon A.: Late Quater-  
639 nary incision rates in the Vésudie catchment area (Southern French Alps) from in situ-produced <sup>36</sup>Cl cosmogenic  
640 nuclide dating: Tectonic and climatic implications, *J. Geophys. Res. Earth Surf.*, 119, 1121–1135, doi:10.1002/  
641 2013JF002985. 2014.

642 Sanchis E. et Séranne M.: Structural style and tectonic evolution of a polyphase extensional basin of the Gulf of  
643 Lion passive margin : the Tertiary Alès basin, southern France. *Tectonophysics* 322 (2000) 219-242, doi :  
644 10.1016/S0040-1951(00)00097-4, 2000.

645 Sartégou A.: Évolution morphogénique des Pyrénées orientales: apports des datations de systèmes karstiques  
646 étagés par les nucléides cosmogéniques et la RPE. *Géomorphologie*. Thèse de l'Université de Perpignan.  
647 Français <NNT : 2017PERP0044>. <tel-01708921> , 2017.

648 Sartégou, A., Bourlès, D. L., Blard, P.-H., Braucher, R., Tibari, B., Zimmermann, L., et al. (2018a). Deciphering  
649 landscape evolution with karstic networks\_ A Pyrenean case study. *Quaternary Geochronology*, 43, 12–29.  
650 <http://doi.org/10.1016/j.quageo.2017.09.005>

651 Sartégou A., Mialon A., Thomas S., Giordani A., Lacour Q., Jacquet A., André D., Calmels L., Bourlès D.L.,  
652 Bruxelles L., Braucher R., Leanni L. Et ASTER team.: When TCN meet high school students: deciphering west-  
653 ern Cévennes landscape evolution (Lozère, France) sin g TCN on karstic networks. Poster 4th Nordic Workshop  
654 on Cosmogenic Nuclides. 2018b.

655 Schaller M., von Blanckenburg F., Hovius N. Et Kubik P.W.: Large-scale erosion rates from in situ-produced  
656 cosmogenic nuclides in European river sediments. *Earth and Planetary Science Letters* 188 (2001) 441-458,  
657 2001.

658 Séranne M., Benedicto A., Labaum P., Truffert C. et Pascal G.: Structural style and evolution of the Gulf of  
659 Lion Oligo-Miocene rifting : role of the Pyrenean orogeny. *Marine and Petroleum Geology*, Vol. 12, No. 8, pp.  
660 809-820, 1995.

661 Séranne M., Camus H., Lucazeau F., Barbarand J. et Quinif Y.: Surrection et érosion polyphasées de la Bordure  
662 cévenole. Un exemple de morphogenèse lente. *Bull. Soc. Géol. France*, 2002, t. 173, n°2, pp. 97-112, 2002.

663 Sibuet J.-C., Srivastava S.P. et Spakman W.: Pyrenean orogeny and plate kinematics. *Journal of Geophysical*  
664 *Research: Solid Earth*, Vol 109, doi: 10.1029/2003JB002514 , 2004.

665 Spassov S. et Valet J.-P.: Detrital magnetisations from redeposition experiments of different natural sediments.  
666 *Earth and Planetary Science Letters* 351-352 (2012) 147-157, dog: 10.1016/j.epsl.2012.07.016, 2012

667 Stewart J. and Watts A.B.: Gravity anomalies and spatial variation of flexural rigidity at mountain ranges. *Jour-*  
668 *nal of Geophysical research*, vol 102, no. B3, Pages 5327-5352, march 10, 1997, doi: 10.1029/96JB03664,  
669 1997.

670 Stock G.M., Granger D.E., Sasowsky I.D., Anderson R.S. et Finkel R.C.: Coomparison of U-Th, paleomag-  
671 netism, and cosmogenic burial methods for dating caves : Implications for landscape evolution studies. *Earth en*  
672 *Planetary Science Letters* 236 (2005) 388-403, doi : 10.1016/j.epsl.2005.04.024, 2005.

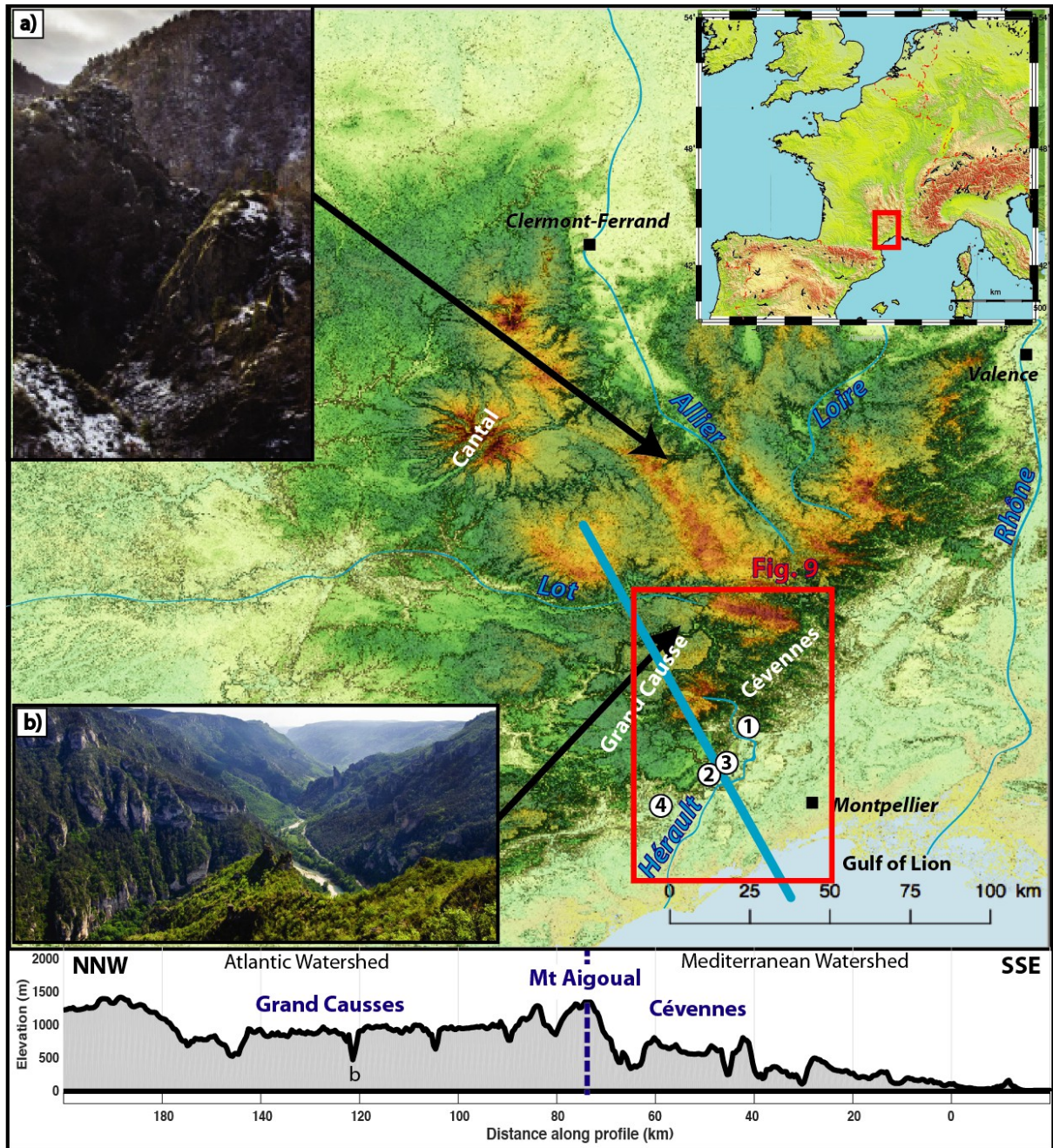
673 Tarayoun A., Mazzotti S., Gueydan F., Quantitative impact of structural inheritance on present-day deformation  
674 and seismicity concentration in intraplate deformation zones, *Earth and Planetary Science Letters*, Volume 518,  
675 2019, Pages 160-171, ISSN 0012-821X, doi: 10.1016/j.epsl.2019.04.043., 2017.

676 Tassy A., Mocochain L., Bellier O., Braucher R., Gattacceca J., Bourlès D.: Coupling cosmogenic dating and  
677 magnetostratigraphy to constrain the chronological evolution of peri-Mediterranean karsts during the Messinian  
678 an the Pliocene: Example of Ardèche Valley, Southern France. *Geomorphology*, 189 (2013), pp. 81-92, doi:  
679 10.1016/j.geomorph.2013.01.019, 2013.

680 Tauxe L., Steindorf J.L. et Harris A.: Depositional remanent magnetisation: Toward an improved theatrical and  
681 experimental foundation. *Earth and Planetary Science Letters* 244 (2006) 515-529, doi:  
682 10.1016/J.epsl.2006.02.003, 2006.

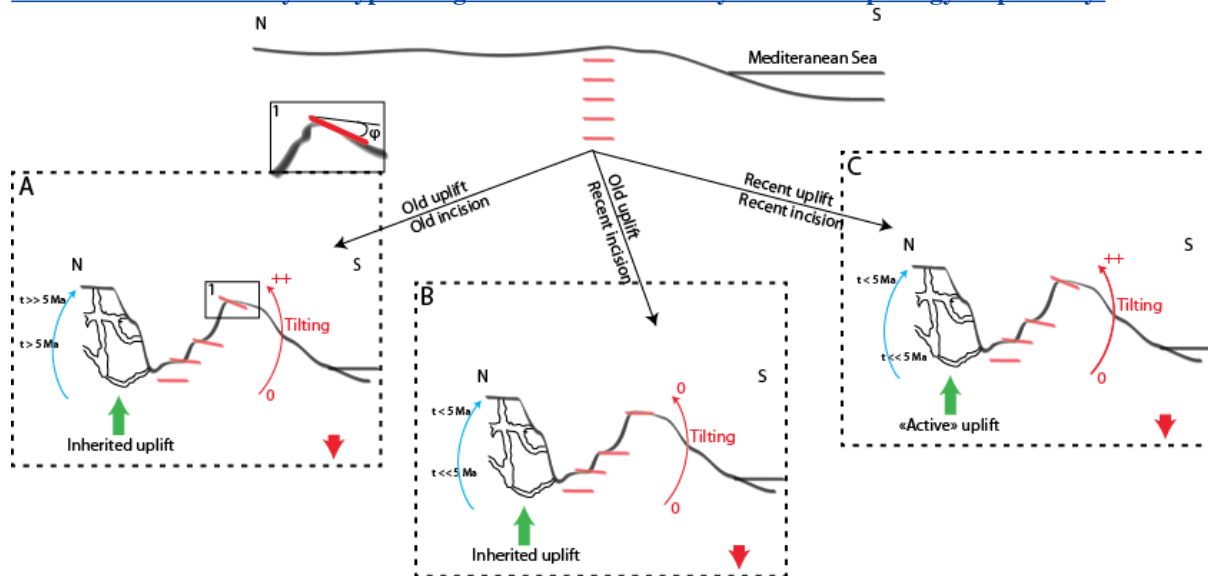
683 Tricart P. : From passive margin to continental collision: A tectonic scenario for the western Alps. *American*  
684 *journal of science*, Vol. 284, February, 1984, P97-120, 1984.

685 Vernant, P., Hivert, F., Chéry, J., Steer, P., Cattin, R., & Rigo, A. (2013). Erosion-induced isostatic rebound  
686 triggers extension in low convergent mountain ranges. *Geology*, 41(4), 467–470.  
687 <http://doi.org/10.1130/G33942.1>



688 morphology respectively. dissected by canyon, and the rugged area with steep valley called the Cevenne.  
 689 They are typical regional limestone and crystalline Note the south-western area with large plateau with

690 dated basaltic flows. Bottom panel is an example of typical topographic profile used for numerical model  
 691 set up.  
 692 (43,669°N; 3.382°E) and 4) is the Lodève basin (43,669°N; 3.382°E) where paleomagnetic analysis have been  
 693 done (43,835°N; 3.616°E) the Garrel Cave system 3) is and (43,819°N; 3.56°E), the Leicasse Cave  
 694 Systems are 1 and 3), 2) where TCN measurements have been done (43,958°N; 3.709°E) and numerated  
 695 site 1) is the Rieutord Canyon (Seuge Canyon) and b) limestone plateau (Tarn Canyon) Location  
 696 of the restricted studied area in red box (fig. 9) and numerated site 1) is  
 697 Figure 1: 30 m resolution DEM of the French Massif-Central and slope shadowed. Examples of finite inci-  
 698 sion typical of the French Massif-Central in a)  
 699 Figure 1: 30 m resolution DEM of the French Massif-Central and slope shadowed. Examples of finite  
 700 incision typical of the French Massif-Central in a) crystalline area (Seuge Canyon) and b) limestone  
 701 plateau (Tarn Canyon) Location of the restricted studied area in red box (fig. 9) and numerated site 1) is  
 702 the Rieutord Canyon (43,958°N; 3.709°E) where TCN measurements have been done, 2) and 3) are the  
 703 Leicasse Cave System (43,819°N; 3.56°E), and the Garrel Cave system (43,835°N; 3.616°E) respectively,  
 704 where paleomagnetic analysis have been done and 4) is the Lodève basin (43,669°N; 3.382°E) with dated  
 705 basaltic flows. Bottom panel is an example of typical topographic profile used for numerical model set up.  
 706 Note the south-western area with large plateau dissected by canyon, and the rugged area with steep valley  
 707 called the Cevenne. They are typical regional limestone and crystalline morphology respectively.



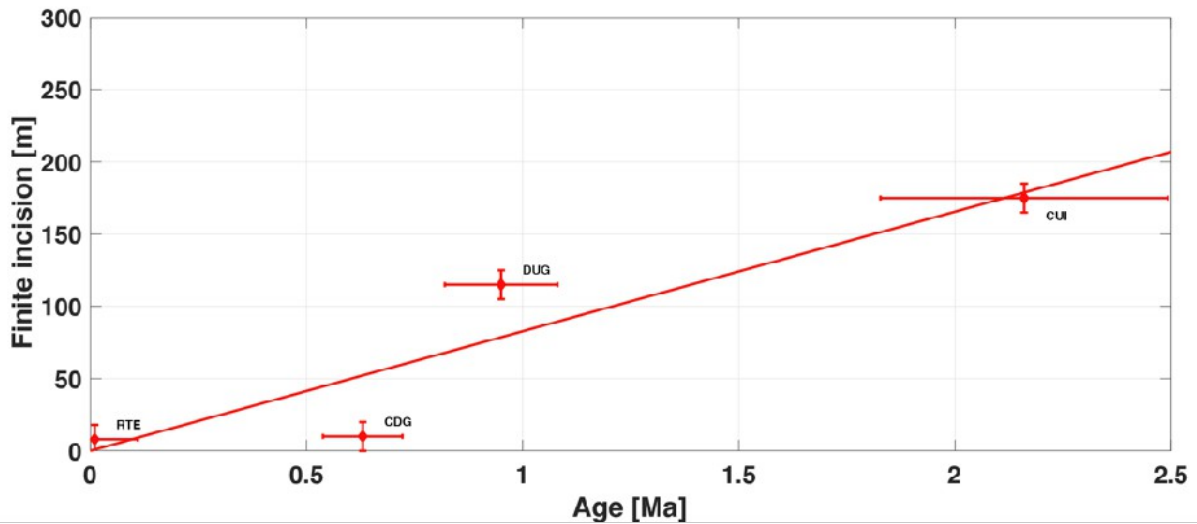
708 Figure 2: conceptual models for landscape evolution. Top panel is the initial stage (prior to uplift). Each  
 709 panel represent a possible scenario explaining current morphology: A) Old uplift and old incision, B) Old  
 710 uplift and recent incision and C) both recent uplift and incision. Blue arrow and associated ages show ex-  
 711 pected result (or absence of) for burial dating. Red level represents morphological markers that are fos-  
 712 silised when reaching the surface, accumulating afterward (or not) the differential uplift by finite tilting.



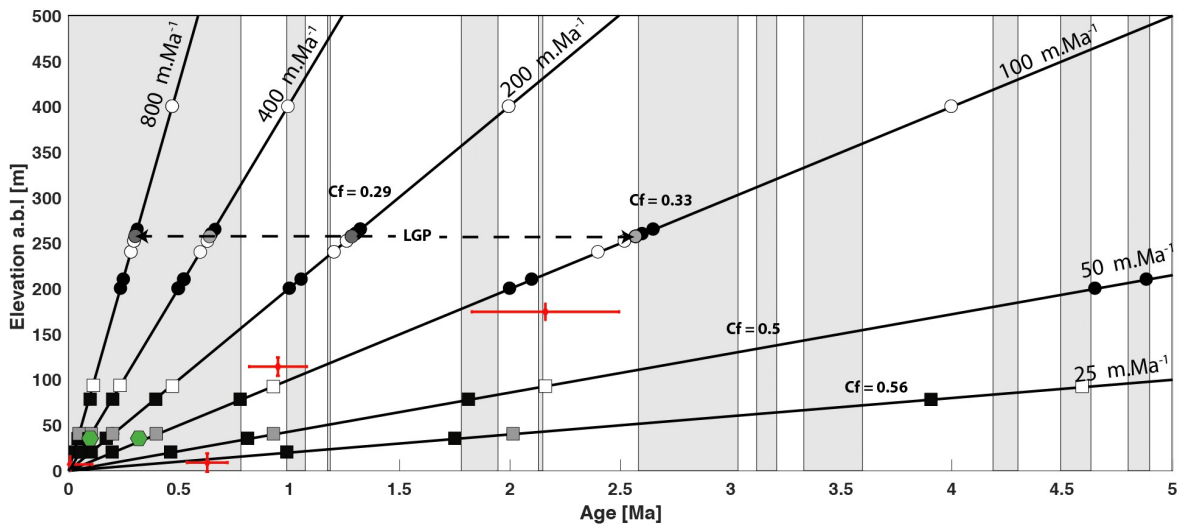
713 | **Figure 3: Example of quartz cobbles sampled for burial dating. Location: Cuillère Cave**



714 | **Figure 4: Example of clay sampling for the paleomagnetic study. Location at the entrance shaft (Highest**  
715 | **elevation of every samples (~580 m a.s.l.), Leicasse Cave system)**

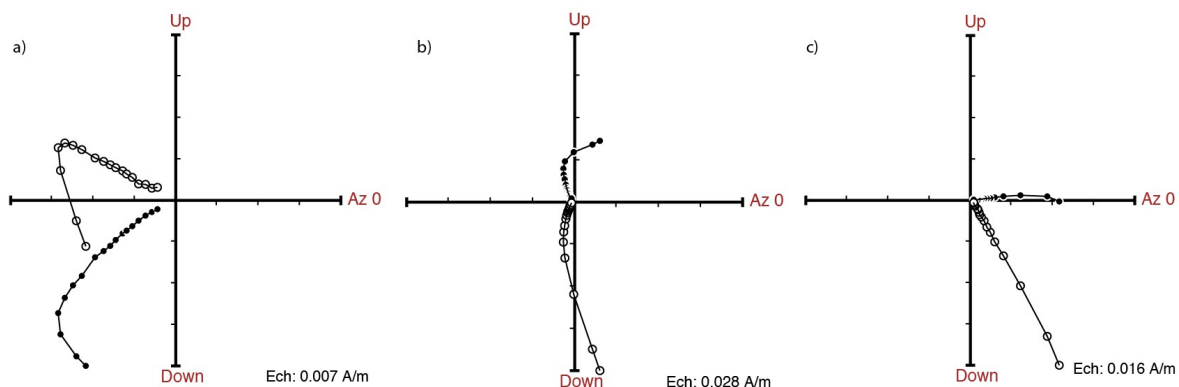


716 **Figure 5: Relation finite incision-burial age for the Rieutord canyon. Finite incision is the elevation of the**  
 717 **sampling site relatively to the current riverbed. RTE for Route Cave, CDG for Camp de Guerre Cave,**  
 718 **DUG for Dugou Cave and CUI for Cuillère Cave**

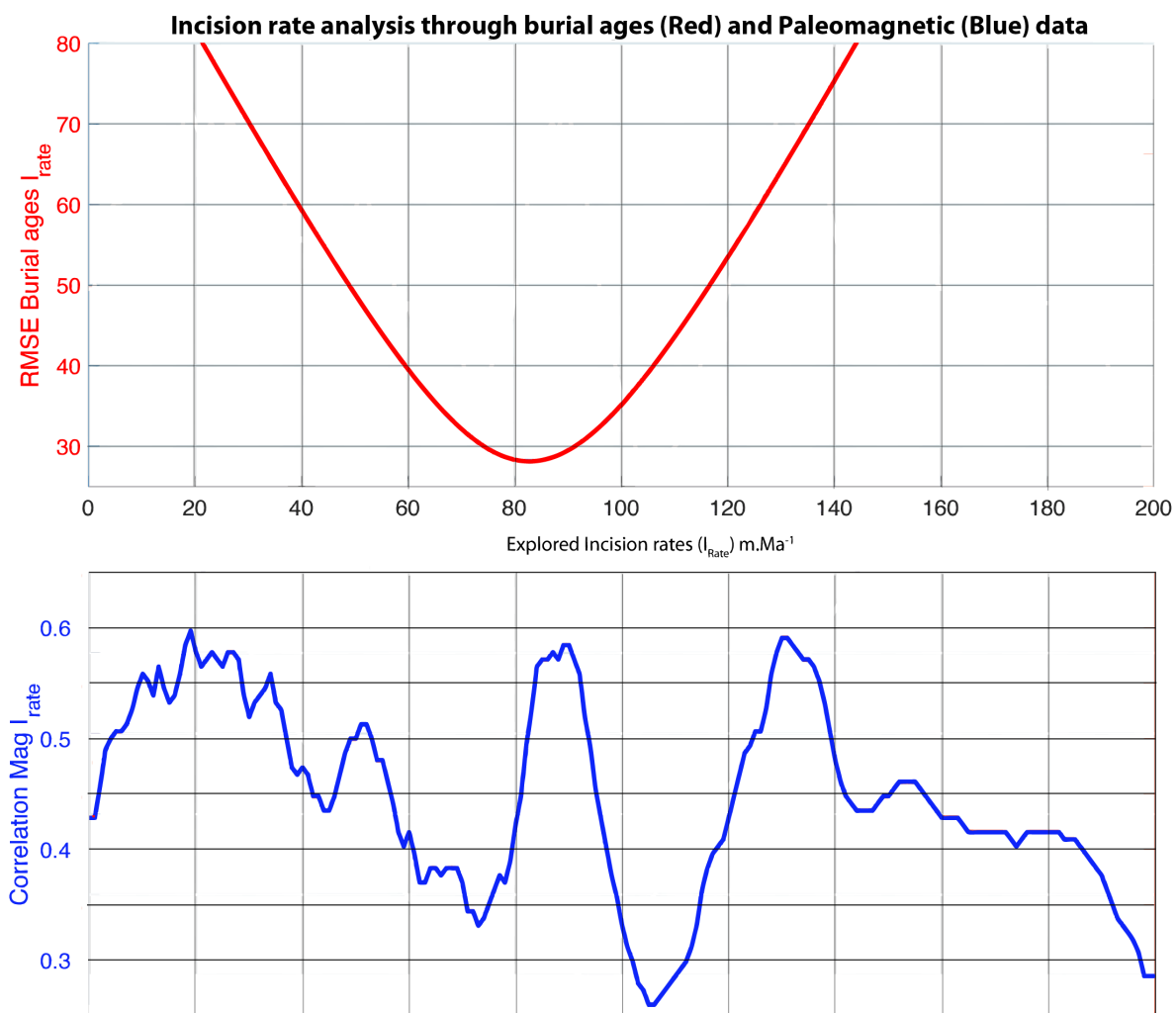


719 **Figure 6: Constraint on the incision rate from plural data set. Circles (Leicasse Cave system) and squares**  
 720 **(Garrel Cave system) are paleomagnetic polarities from clay deposits. Black is for Normal polarity, white**  
 721 **for Reversed polarity and grey for transitional signal.**  
 722 **Each point is representative of one sampling profile including an average of 10 samples per site. Lines**  
 723 **represent different linear incision rates with example of good correlation (red ones) and bad correlation**  
 724 **(black ones). The horizontal dashed line shows the predicted polarities-age for one site located ~100m**  
 725 **a.b.l. This measured reversed polarity match with theoretical red lines but fails with the three other**  
 726 **exposed incision rate.**  
 727 **Green hexagons are representation of U/Th ages obtain in the Garrel (Camus, 2003). Burial ages from fig.**  
 728 **4 are shown for comparison (Red points)Figure 6. Constraining the incision rate in the Cevennes margin,**  
 729 **using paleomagnetic polarities from clay deposits (black, grey and white symbols) and burial ages (red crosses):**  
 730 **Circles are from the Leicasse cave with LGP being *les gours sur pattes* profile (see text), squares are from the**  
 731 **Garrel cave. Black, grey and white symbols correspond to normal, transitional and reverse polarities,**  
 732 **respectively. Black linear straight lines define possible incision rates that are supposed stable thought time.**

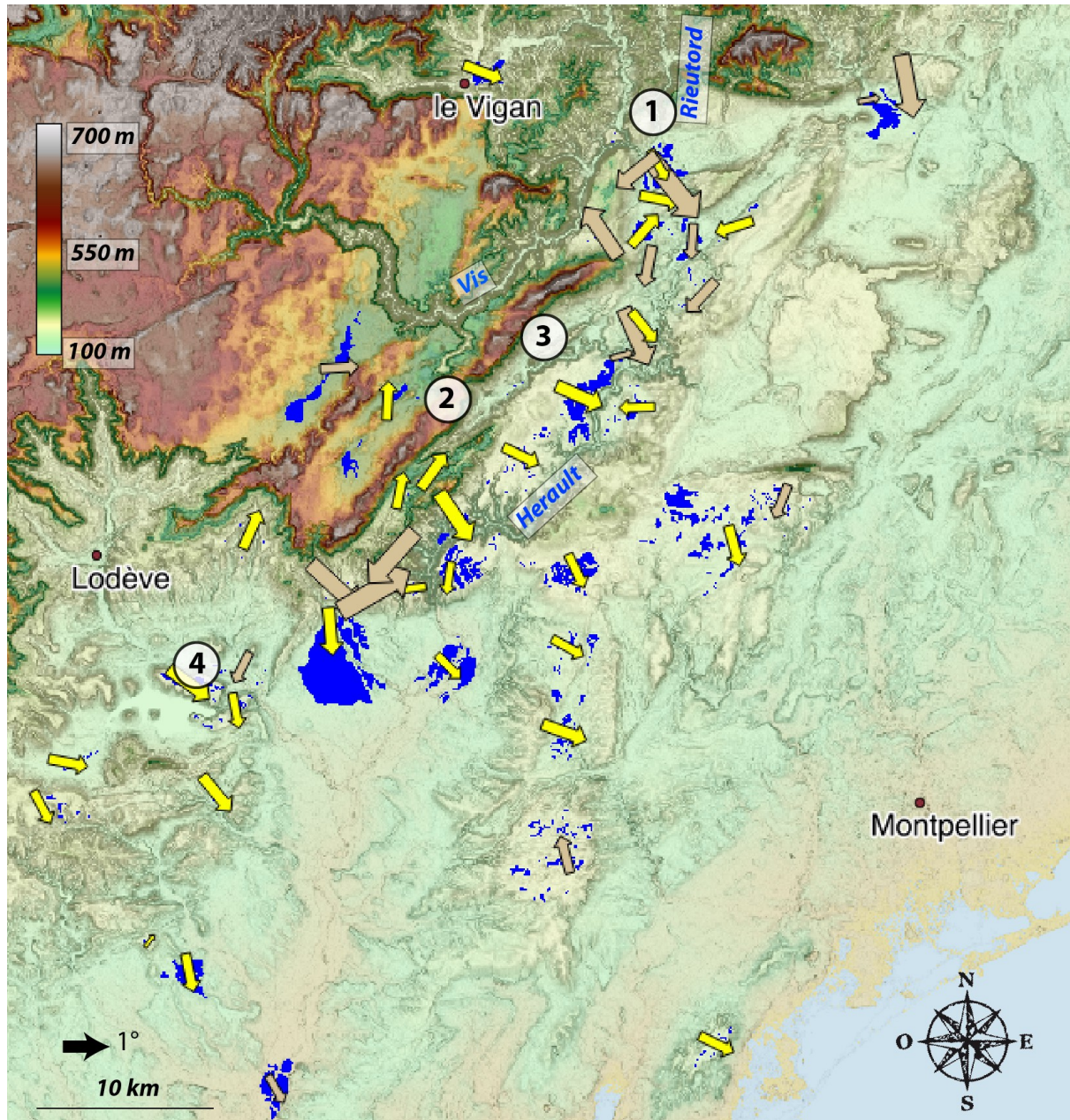
733 | (numbers in white rectangles define the  $C_f$  values are  $C$  correlation factor between the measured paleomagnetic  
 734 | polarities and the predicted paleomagnetic scale (see also Figure 8). Green hexagons show the U/Th ages  
 735 | obtained in the Garrel by Camus (2003).



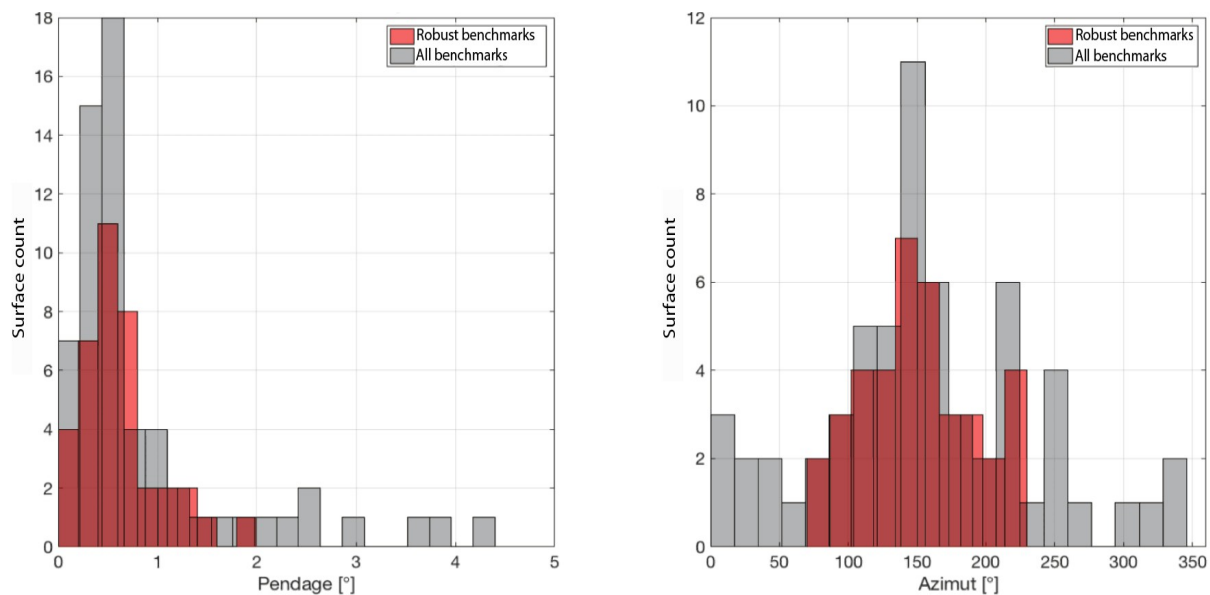
736 **Figure 7: Zijderveld Diagram for three samples from the Gours-sur-Pattes (Leicasse) site. Stratigraphical**  
 737 **order is from a) (the older, base of the profile) to c) (the younger, top of the profile).**



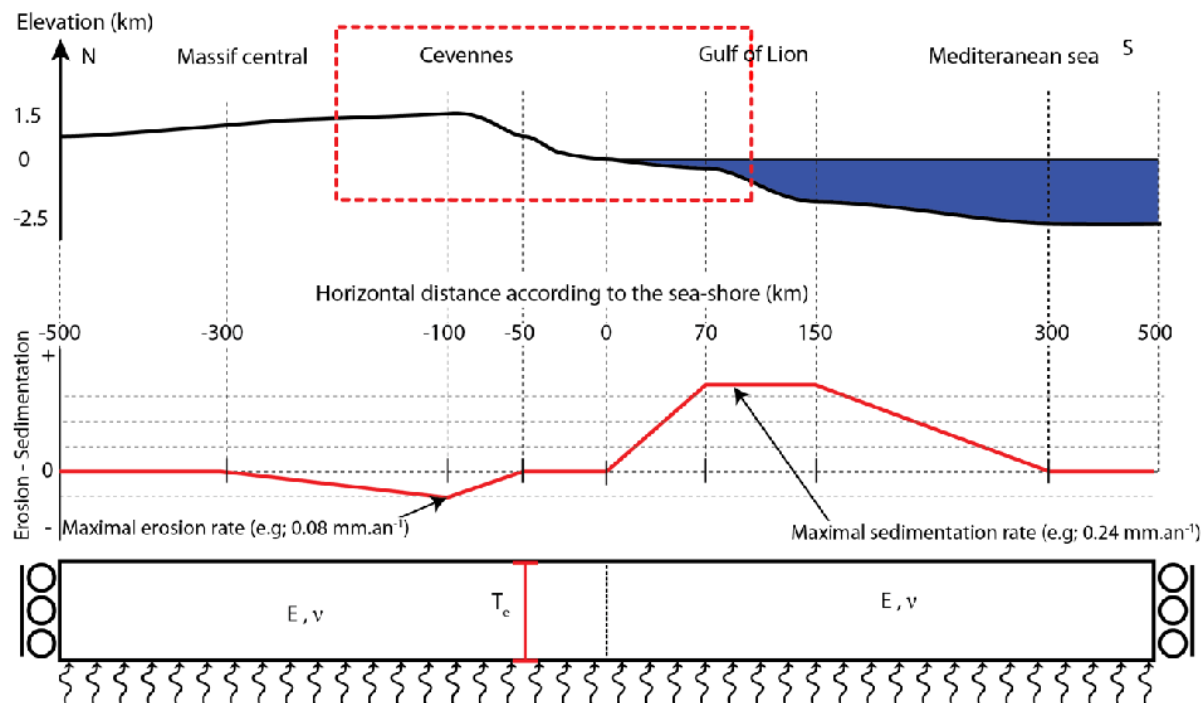
738 | **Figure 8: Best incision rate based on paleomagnetic data (blueRed) and burial ages (blueRed). The**  
739 | **blueRed curve is the normalised smoothed (10 m/Ma sliding window for better visualisation) correlation**  
740 | **between theoretical and observed polarities. The highest correlation corresponds to the best incision**  
741 | **rates. The redblue curve is the RMSE for the linear regression through the burial ages data set shown on**  
742 | **Fig. 4.**



743 **Figure 9: Tilting map of geomorphological benchmark (yellowblue areas). Fond-map is 305 m resolution**  
 744 **DEM with slope shadow. Red Arrows are orientating according to the marker downward dip and sized**  
 745 **according to the corrected tilting angle (the bigger, the more the tilting). Yellow and brown arrows are**  
 746 **for robust and rejected surfaces respectively. Several arrows are hidden because of their small size and**  
 747 **too high proximity with bigger ones. Numerated site 1) is the Rieutord Canyon, 2) is the Leicasse Cave**  
 748 **System, 3) is the Garrel Cave system and 4) is the Lodève basin with dated basaltic flows. See Fig. 1 for**  
 749 **geographical coordinates.**

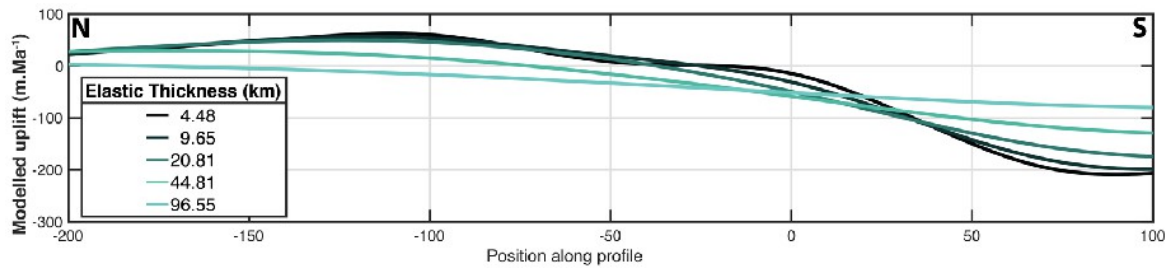


750 **Figure 10: Tilting and azimuth distribution.** Left panel is density distribution for surface maximum  
 751 **tilting in degree.** Right panel is azimuth of maximum dipping relative to the north. For each histogram,  
 752 **red and grey populations are for robust and primary detected markers.**

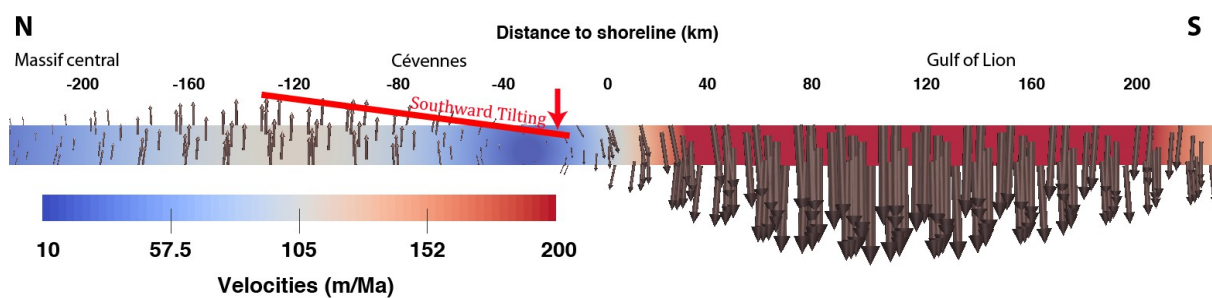


753 **Figure 11: Top panel: schematic topographic profile.** ~~is delimited by zones studied~~  
 754 ~~The studied area that~~ **includes the T** ~~the red box~~ **delimites the area shown fig. 1 and 9 (ef fig. 1).** Middle panel, surface processes  
 755 **profile, negative values are for erosion and positive values for sedimentation.** Bottom panel: model set-up

756 with two compartments (one for the Cevennes area and the second on for the gulf of lion). The base of the  
 757 model is compensated in pressure and the right and left limits are fixed at zero horizontal velocities and  
 758 free vertical ones.  $T_e$  is the equivalent elastic thickness (in km),  $E$  (Pa) and  $\nu$  are the Young modulus  
 759 and the Poisson coefficient respectively whom values are independent in each compartment.



760 Figure 12: Modelled uplift according to different  $T_e$ . Most probable  $T_e$  are between 10 and 30 km.



761 Figure 13: Modelling result for  $T_e=15$ km. Erosion-sedimentation rate profile is the same as in fig. 6.  
 762 Velocity field is shown using arrow for scale and orientation and colour code for value. Black values on  
 763 top are distance relative to the sea-shore (positive value landward and negative values seaward). Red line  
 764 represent the southward modelled tilting due to differential uplift.

Cave	Lat	Lon	Elevation	height (a.b.l.)	$^{10}\text{Be}$ conc (atom/g)	$\sigma$ $^{10}\text{Be}$ (atom/g)	$^{26}\text{Al}$ conc (atom/g)	$\sigma$ $^{26}\text{Al}$ (atom/g)	$^{26}\text{Al}/^{10}\text{Be}$ (and error)	Burial age (Ma)	Burial age error (Ma)
RTE	43,960	3,707	175	8	3,54E+04	1,18E+03	2,16E+05	1,47E+04	6,11 +/-0.46	0,20	+0.16/-0.15
CDG	43,955	3,710	185	10	8,87E+04	3,12E+03	4,29E+05	3,28E+04	4,83 +/-0.41	0,67	+0.18/-0.16
DUG	43,957	3,711	245	115	1,27E+04	5,68E+02	5,29E+04	6,36E+03	4,15 +/-0.53	0,99	+0.28/-0.25
CUI	43,959	3,711	354	175	1,70E+04	7,14E+02	3,75E+04	5,28E+03	2,20 +/-0.32	2,28	+0.33/-0.28

765 Table 1: Samples analytical results and parameters. Cave code are: RTE for the “de la route” Cave, CDG for the  
 766 “Camp de Guerre” cave, DUG for the “Dugou” Cave and CUI for the “Cuillère” Cave. Main parameters are the  
 767 geographical coordinate (Lat, Lon in decimals degree), the elevation (a.s.l), the height (a.b.l., computed relative-  
 768 ly to the surface river elevation. The concentration (atoms/g quartz) of  $^{10}\text{Be}$  and  $^{26}\text{Al}$  in collected sand samples  
 769 are all AMS  $^{10}\text{Be}/\text{Be}$  and  $^{26}\text{Al}/\text{Al}$  isotopic ratios corrected for full procedural chemistry blanks and normalised  
 770 to KN-5-4 and KN -4-2, respectively. The error () is for total analytical error in final average  $^{10}\text{Be}$  and  $^{26}\text{Al}$

771 concentrations based on statistical counting error s in final  $^{10}\text{Be}/\text{Be}$  ( $^{26}\text{Al}/\text{Al}$ ) ratios measured by AMS in  
772 quadrature with a 1% error in  $^9\text{Be}$  spike concentration (or a 4% error in  $^{27}\text{Al}$  assay in quartz) and a 2% (or  
773 3%) reproducibility error based on repeat of AMS standards. Burial age (minimum) assuming no post-burial  
774 production by muons at given depth (all deeper than 30m) in cave below surface and assuming initial  
775  $^{26}\text{Al}/^{10}\text{Be}$  ratio is given by the production ratio of 6.75. The burial age error determined by using a  $\pm 1\sigma$   
776 range in the measured  $^{26}\text{Al}/^{10}\text{Be}$  ratio